Full-Scale Hydrogen Mitigation Installation and Testing at Nevada Solar One

Greg Glatzmaier and Koenraad Beckers

National Renewable Energy Laboratory

NREL is a national laboratory of the U.S. Department of Energy
Office of Energy Efficiency & Renewable Energy
Operated by the Alliance for Sustainable Energy, LLC

This report is available at no cost from the National Renewable Energy Laboratory (NREL) at www.nrel.gov/publications.

Contract No. DE-AC36-08GO28308

Technical Report
NREL/TP-5700-81867
June 2022

Full-Scale Hydrogen Mitigation Installation and Testing at Nevada Solar One

Greg Glatzmaier and Koenraad Beckers

National Renewable Energy Laboratory

Suggested Citation
Glatzmaier, Greg, and Koenraad Beckers. 2022. *Full-Scale Hydrogen Mitigation Installation and Testing at Nevada Solar One*. Golden, CO: National Renewable Energy Laboratory. NREL/TP-5700-81867. https://www.nrel.gov/docs/fy22osti/81867.pdf

NREL is a national laboratory of the U.S. Department of Energy
Office of Energy Efficiency & Renewable Energy
Operated by the Alliance for Sustainable Energy, LLC

This report is available at no cost from the National Renewable Energy Laboratory (NREL) at www.nrel.gov/publications.

Contract No. DE-AC36-08GO28308

Technical Report
NREL/TP-5700-81867
June 2022

National Renewable Energy Laboratory
15013 Denver West Parkway
Golden, CO 80401
303-275-3000 • www.nrel.gov

NOTICE

This work was authored by the National Renewable Energy Laboratory, operated by Alliance for Sustainable Energy, LLC, for the U.S. Department of Energy (DOE) under Contract No. DE-AC36-08GO28308. Funding provided by the U.S. Department of Energy Office of Energy Efficiency and Renewable Energy Building Technologies Office. The views expressed herein do not necessarily represent the views of the DOE or the U.S. Government.

This report is available at no cost from the National Renewable Energy Laboratory (NREL) at www.nrel.gov/publications.

U.S. Department of Energy (DOE) reports produced after 1991 and a growing number of pre-1991 documents are available free via www.OSTI.gov.

Cover Photos by Dennis Schroeder: (clockwise, left to right) NREL 51934, NREL 45897, NREL 42160, NREL 45891, NREL 48097, NREL 46526.

NREL prints on paper that contains recycled content.

Preface

This report describes the U.S. Department of Energy's Technology Commercialization Fund CRADA project #34657 between the National Renewable Energy Laboratory and Acciona Energy. The project period was from November 1, 2018, through December 31, 2021.

This report is available at no cost from the National Renewable Energy Laboratory at www.nrel.gov/publications.

List of Acronyms

AE	Acciona Energy USA, Inc.
CRADA	Cooperative Research and Development Agreement
CSP	concentrating solar power
DOE	U.S. Department of Energy
EPC	engineering, procurement, and construction
HSG	headspace gas
HTF	heat transfer fluid (Dowtherm ATM or Therminol VP-1TM)
KOP	knockout pot
NREL	National Renewable Energy Laboratory
NSO	Nevada Solar One
PI	principal investigator
PLC	programmable logic controller
SCA	solar collector assembly
SETO	Solar Energy Technologies Office
TCF	Technology Commercialization Fund
TRL	technology readiness level
VFD	variable frequency drive

This report is available at no cost from the National Renewable Energy Laboratory at www.nrel.gov/publications.

Table of Contents

Executive Summary 1
1 TCF Project Objective 4
2 TCF Project Background 4
3 Previous NREL Work Relating to a Hydrogen Mitigation Solution 8
4 TCF Project Technology Development Approach 9
5 TCF Project Tasks and Results 11
6 TCF Project Continuing Work 43
7 TCF Project Summary 43
References 45

This report is available at no cost from the National Renewable Energy Laboratory at www.nrel.gov/publications.

List of Figures

Figure 1. Parabolic trough power plant components that contain circulating HTF 4
Figure 2. Parabolic reflectors with receivers at their focal line 5
Figure 3. Hydrogen transport in a receiver 6
Figure 4. Steps to model and determine process rates 10
Figure 5. Hourly distribution of temperature in °F and pressure in psig for the NSO expansion tank headspace gas in 2017. Numbers in each temperature/pressure condition are the total hours that condition occurred in 2017 12
Figure 6. Existing and new piping for the test-scale process layout 13
Figure 7. 3D assembled piping and equipment layout on the process platform 13
Figure 8. Insulation thickness and heat trace power for piping, module, and KOP—insulated piping is shown in blue 15
Figure 9. Schematic diagram of mitigation process with five heat trace circuits color-coded and labeled 17
Figure 10. Membrane insert components including membrane assembly 17
Figure 11. Welded insert and membrane components 18
Figure 12. Separation module and palladium membrane testing at NREL 19
Figure 13. Heat trace and insulation added to separation module at NSO 20
Figure 14. KOP showing locations of vortex breaker and MLI 21
Figure 15. Design and location of vortex breaker in bottom of KOP 21
Figure 16. Design and location of MLI with level switches 22
Figure 17. Compressor power versus process gas volumetric flowrate—power requirement due to flowing process gas through piping and valves 23
Figure 18. Catalytic oxidizer with four catalysts in series and inlet gas preheating 25
Figure 19. Catalytic oxidizer during testing at NREL 25
Figure 20. Manifold layout for ½” tubing 27
Figure 21. Schematic of sensor and communication wiring from PLC to platform 28
Figure 22. Schematic of sensor and communication wiring from PLC to junction boxes on the process platform 28
Figure 23. Circuit for conditioning level switch states and controlling drain valve 29
Figure 24. Control circuit for sending a signal to the electronic pressure regulator to supply nitrogen gas pressure to the compressor shaft seal 30
Figure 25. 480V and 240V current requirements for process installation 31
Figure 26. Standby and operating modes for PLC process control 32
Figure 27. Power plant components in which the plant model calculates hourly HTF hydrogen levels for each month of the year 33
Figure 28. Comparison of degradation rates of new HTF, and benzene at HTF temperatures from 300°C to 400°C 35
Figure 29. Hourly hydrogen levels in HTF flowing through SCA 8 receivers; model assumes HTF with 1.4% benzene-like derivatives, and no hydrogen extraction 36
Figure 30. Hourly hydrogen levels in HTF flowing through SCA 8 receivers; model assumes HTF with 1.4% benzene-like derivatives, and with hydrogen extraction 37
Figure 31. Average monthly hydrogen levels in HTF flowing through SCA 8 receivers (model assumes HTF with 1.4% benzene-like derivatives) with and without hydrogen extraction 38
Figure 32. Annual hydrogen levels in SCA 2, 4, 6, and 8 receiver annulus—no hydrogen extraction 38
Figure 33. Annual hydrogen levels in SCA 2, 4, 6, and 8 receiver annulus—with hydrogen extraction 39
Figure 34. Permeate pressure versus time for measuring hydrogen in the module after treating the membrane with 5% hydrogen in nitrogen 41
Figure 35. Catalytic oxidizer temperature response when hydrogen is withdrawn from the permeate volume and passed through the oxidizer 42

This report is available at no cost from the National Renewable Energy Laboratory at www.nrel.gov/publications.

List of Tables

Table 1. Summary of heat transfer calculation results for worst-case scenario (10 m/s wind velocity, -18°C ambient temperature, 300°C HSG temperature, 100 psig HSG pressure, 200 ACFM flow rate) 16
Table 2. Summary of hydrogen flow test conditions and resulting hydrogen conversion 26
Table 3. Electrical requirements for 480V power 30
Table 4. Electrical requirements for 240V power 31

This report is available at no cost from the National Renewable Energy Laboratory at www.nrel.gov/publications.

Executive Summary

This Technology Commercialization Fund (TCF) project was preceded by an original Cooperative Research and Development Agreement (CRADA) between the National Renewable Energy Laboratory (NREL) and Acciona Energy USA (AE). The purpose of that CRADA was to identify and develop a method that would mitigate the problem of hydrogen buildup in the circulating heat transfer fluid (HTF) of parabolic trough power plants. This original work began with power plant, process, and receiver modeling that was followed by an extensive experimental effort at NREL. The key outcome was the development and laboratory demonstration of an integrated process module that extracts hydrogen from a gas mixture and measures the partial pressure and molar extraction rate of hydrogen. Advances realized in this first CRADA were:

- A simple hydrogen sensor that measures hydrogen partial pressure in the expansion tank headspace gas at expansion tank conditions
- Extended receiver heating and heat loss measurements that provided the first evidence that hydrogen permeation in receivers is reversible and that receiver performance can be improved with extended receiver heating when no hydrogen is present in the absorber
- A power plant hydrogen transport and generation model that showed that controlling hydrogen levels in the expansion tanks maintains the level of dissolved hydrogen in the HTF that is circulating in the collector field to target levels
- A receiver lifetime model that estimated the years that a receiver would last in the collector field as a function of solar collector assembly (SCA) position and dissolved hydrogen concentration in the circulating HTF
- Modeling and experimental testing that generated critical partitioning and mass transfer coefficients for hydrogen at the HTF liquid/gas interface within the expansion tanks
- An integrated hydrogen separator and sensor module design that separates hydrogen from the headspace gas, measures hydrogen partial pressure in the headspace gas, and measures the molar rate of hydrogen extraction from the expansion tank headspace gas.

This report details the findings of a more recent TCF-funded project, which was also performed under a CRADA between NREL and AE. The objectives of this TCF CRADA were to design, engineer, procure, and install the hydrogen mitigation process that was developed during the first CRADA at the Nevada Solar One (NSO) power plant near Boulder City, Nevada. Following installation, the process was to be commissioned and operated as part of regular daily operations at the NSO power plant. The advances achieved in the first CRADA served as the design basis for the process installation that was conducted during the second CRADA. In this way, all effort that was made in the first CRADA was used to advance and complete the development of this technology in the second TCF CRADA.

At the start of this TCF project, NREL and NSO staff met to layout plans for completing the process installation and operation at the NSO power plant. The goal of this project was challenging, and the risk for failure was significant. This was to be the first installation of this technology at any parabolic trough power plant. The process needed to be scaled to commercial size from laboratory experiments that were performed at NREL during the first CRADA between NREL and AE.

This report is available at no cost from the National Renewable Energy Laboratory at www.nrel.gov/publications.

NREL and NSO initially decided to proceed with a two-step approach. First, the process would be installed at a test scale. This scale would confirm the performance of all the process components and determine the final specification for the second, full-scale installation. As NREL and NSO proceeded with the test-scale installation, AE realized that the time, effort, and cost that would be needed for the test-scale installation was as much as they had available for the whole project. To address this issue, we proceeded with a combined process installation in which the knockout pot (KOP), process piping, separation module, control valves, sensors, signal and power wiring, and programmable logic controller (PLC) were purchased and installed at full process scale. To keep costs within reason, we stayed with the test-scale size for the separation module, headspace gas compressor, and vacuum pumps. If the installed process did not meet their long-term performance targets, AE had options to (1) install two higher-performance turbopumps, (2) purchase and install a headspace gas blower with higher volumetric pumping capacity, and (3) install a second separation module.

NREL and NSO identified a location for the process installation that was at ground level on the concrete secondary containment pad and below the two south expansion tanks. We identified access to the headspace gas in the expansion tanks by connecting supply and return piping to the horizontal nitrogen gas supply line that was located 14 feet above the concrete pad. Process equipment was mounted onto a steel platform that was 2 feet above the concrete pad to protect the equipment from potential flash flooding in the power block.

We identified and procured major equipment including (1) the headspace gas compressor that circulates headspace gas from the expansion tanks to the process and back to the tanks, (2) two vacuum pumps that evacuate hydrogen from the separation module, (3) process piping, (4) isolation valves that protect the process when not operating, (5) control valves that direct process gas flow during operation, (6) temperature, pressure, and flow sensors that monitor process conditions, and (7) the PLC that monitors and controls process functions for automated operation.

Three pieces of equipment needed to be custom designed and fabricated—the KOP that removed HTF condensate from the headspace gas supply flow, the separation module, and the catalytic oxidizer. The KOP and separation module were custom fabricated by Nick's Welding in Denver, Colorado, and were certified as ASME pressure vessels.

The separation module included the palladium/silver alloy membrane and membrane assembly that separates hydrogen from the headspace gas. NREL fabricated the membrane and assembly at its machine shop. NREL tested the membrane assembly and separation module functions before shipping to NSO. The catalytic oxidizer was specified, fabricated, and tested at NREL before shipping to NSO. The KOP was shipped directly to NSO from Nick's Welding in Denver.

All other major equipment, piping, instrumentation, and controls were shipped to NSO and installed. NSO arranged for a contractor to add heat trace and insulation to the process piping and equipment. NSO and NREL performed initial process commissioning by testing equipment and subsystems individually. Complete process operation was demonstrated in February 2020 just before the COVID-19 pandemic forced shutdown of work at NSO due to NREL travel restrictions.

This report is available at no cost from the National Renewable Energy Laboratory at www.nrel.gov/publications.

From March 2020 to March 2021, NREL travel to NSO was limited to two trips. We made hardware and programming improvements, but we did not operate the process during these trips. In April 2021, NREL began making regular trips to NSO. Process operation in April, May, and June was interrupted by several problems related to process startup. In July and August, NREL and NSO modified the process piping and worked through the operational problems to get the process operating on a daily schedule.

NSO operated the process during the fall months of 2021. NREL made two more trips to NSO to measure headspace gas hydrogen. During these months, we were successful in making real-time hydrogen partial pressure measurements in the headspace gas and operating the process on a daily schedule. Measurements in November showed negligible hydrogen in the headspace gas due to shorter days and lower HTF temperatures. These results were consistent with our power plant model that predicted no hydrogen in the headspace gas during November, December, and January.

The project period for this TCF project ended on December 31, 2021, but work continues in 2022 to establish the performance of the process and its impact on the NSO solar field receivers.

This project was difficult to conduct and complete due to its challenging nature and delays caused by the COVID-19 pandemic. Even so, the following are our most notable achievements:

- A process configuration and location that was manageable and did not interfere with the day-to-day operation of the NSO power plant
- Successful procurement of major equipment, instrumentation, and contracting services that met the requirements for installation in a Class I Division II restricted area
- Successful design and third-party fabrication of custom vessels that were certified to meet ASME pressure codes
- First-of-a-kind installation and testing of a complex mitigation process without any safety-related or accident-related events
- Successful completion of process commissioning while managing work delays caused by the COVID-19 pandemic
- First real-time measurements of hydrogen partial pressure in the headspace gas of expansion tanks at a parabolic trough power plant
- A successful collaboration between NREL and NSO staff over a period of several years to complete all design, procurement, installation, and commissioning tasks without help from an engineering, procurement, and construction (EPC) contractor
- Follow-on plans to track the performance of the process that was installed at NSO
- Follow-on plans to license the technology to an engineering services company and to install the same process at power plants in the United States, Spain, North Africa, South Africa, and the Middle East.

This report is available at no cost from the National Renewable Energy Laboratory at www.nrel.gov/publications.

1 TCF Project Objective

This project was performed under a CRADA between NREL and AE. The purpose was to advance an NREL TRL 3 technology that was developed during the previous CRADA from completed laboratory testing to full-scale process installation and testing at AE's Nevada Solar One (NSO) power plant. The project's objective was to complete full-scale implementation and performance verification of the NREL hydrogen mitigation technology at the NSO power plant in Boulder City, Nevada.

2 TCF Project Background

Parabolic trough power plant design and operation

The parabolic trough power plant is a linear focus concentrating solar power (CSP) plant that generates utility-scale electricity from sunlight. Figure 1 shows power plant components that contain circulating HTF. They include the collector field reflectors and receivers, steam generators, and HTF expansion tanks.

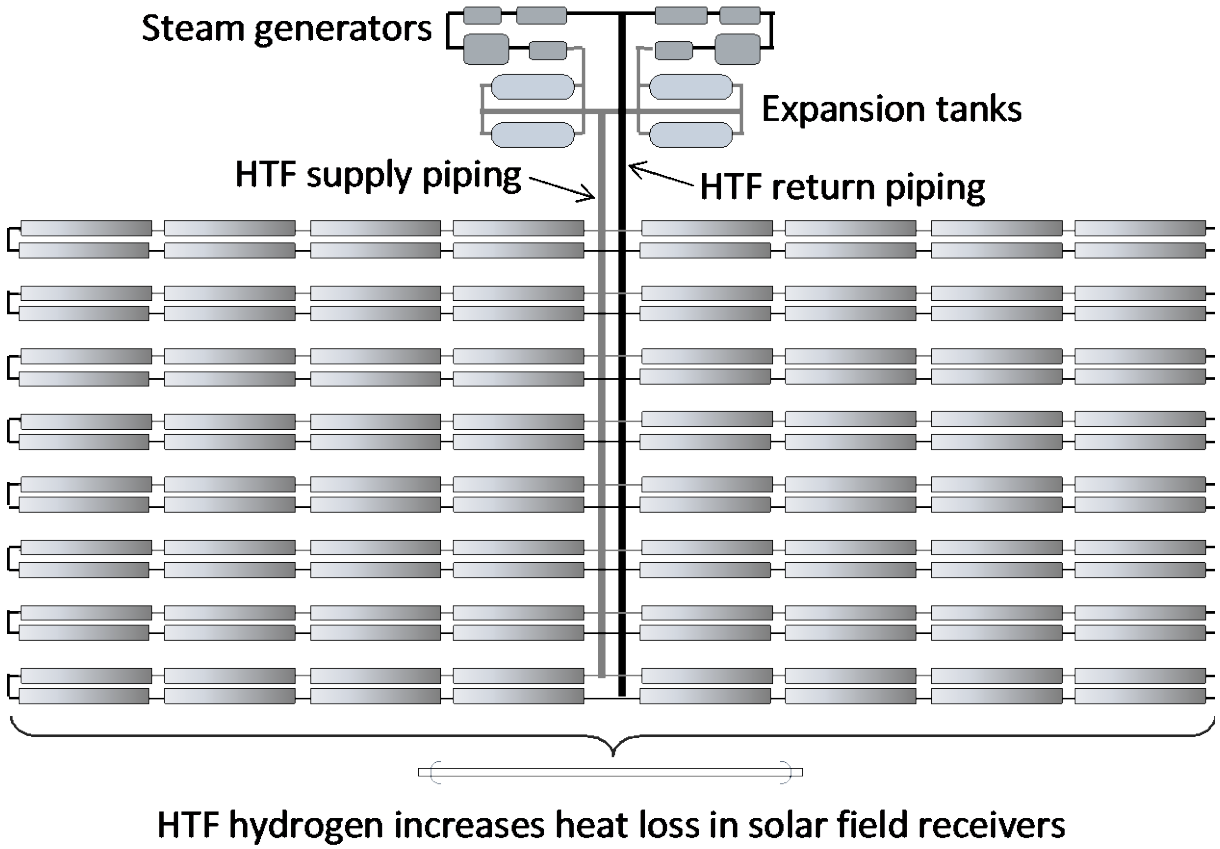

Figure 1. Parabolic trough power plant components that contain circulating HTF

The collector field consists of parabolic reflectors that focus and direct sunlight to receivers, which are located at their focal line as shown in Figure 2. The concentrated sunlight heats the HTF as it flows through the receivers. The HTF produces steam in the steam generators that is

This report is available at no cost from the National Renewable Energy Laboratory at www.nrel.gov/publications.

sent to the turbine to generate electricity for the electric power grid. The expansion tanks hold the HTF inventory that is not in circulation.

Figure 2. Parabolic reflectors with receivers at their focal line

Commercial CSP power plants were first built in the 1980s and have proved to be a reliable source of utility-scale electricity. Currently there are about 80 commercial plants operating worldwide that have a total capacity of 5 GW [1]. All commercial plants use an HTF that is a mixture of two hydrocarbons—biphenyl and diphenylether. The HTF is stored at 150°C to 293°C in the expansion tanks (Figure 1). From there, it flows through the supply piping to the collector field, where it flows through receivers and is heated by sunlight to its upper operating temperature of 393°C. The HTF flows back through the return piping to the steam generators, where it drops its temperature to 293°C before returning to the expansion tanks. Some power plants include a second flow loop in which the HTF heats a molten salt that functions as the thermal storage medium. This storage fluid can generate steam at a later time, and thus allows the power plant to generate electricity during times when sunlight is not available.

Problem description

Near its upper operating temperature (393°C), the HTF degrades slowly to generate hydrogen gas. The degradation reactions include polymerization of biphenyl and intramolecular ring closure of the diphenylether [2]. Both reactions are due to cleavage of carbon-hydrogen bonds within their components [3], and both have an Arrhenius temperature dependence that causes these rates to be negligible at 293°C and very significant near 393°C in terms of hydrogen generation.

The reactions produce small concentrations (ppb levels) of dissolved hydrogen that circulates with the HTF throughout the collector field, steam generators, and expansion tanks. Practically, degradation is not inhibited by the presence of hydrogen in the HTF, so the hydrogen generation rate depends only on HTF temperature and is greatest when the HTF is near its upper operating temperature. Dissolved hydrogen concentrations would increase to high pressures except for permeation of hydrogen through the plant piping and process equipment walls that causes

This report is available at no cost from the National Renewable Energy Laboratory at www.nrel.gov/publications.

dissolved hydrogen to reach a quasi steady-state concentration. Piping and process equipment are composed of carbon steel, which is permeable to hydrogen [4, 5]. Its permeability also has an Arrhenius temperature dependence. At any time, the dissolved hydrogen concentration balances the plant-wide hydrogen generation rate with the plant-wide hydrogen permeation rate out of the plant via piping and process equipment walls.

Figure 3 shows the receiver—the component that absorbs concentrated sunlight from the reflector and heats the HTF to 393°C. The receiver consists of a stainless steel tube, called the absorber, through which flows the HTF. The absorber is surrounded by a glass tube that seals to the absorber on both ends. The enclosed annulus is evacuated to eliminate conduction and convection from the absorber. The receiver functions as a thermos, allowing concentrated sunlight to pass through the glass to the absorber minimizing heat loss from the receiver.

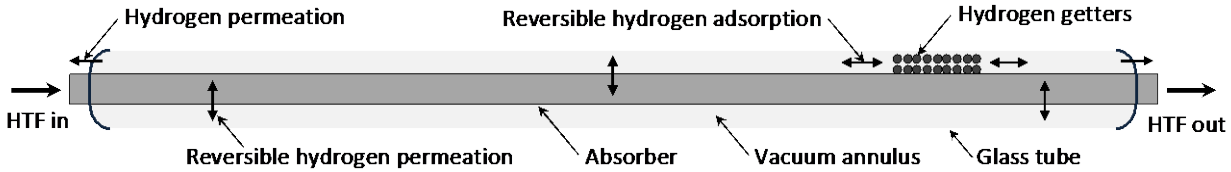

Figure 3. Hydrogen transport in a receiver

In the collector field, dissolved hydrogen in the HTF permeates across the absorber tube wall and into the receiver's evacuated annulus (Figure 3). Due to its high thermal conductivity, the presence of small hydrogen pressures (1 mbar) causes a significant increase in the receiver's heat loss. The increased heat loss reduces the thermal efficiency of the collector field, and ultimately reduces electricity production by the power plant.

During the first several years of plant operation, hydrogen in the annulus is absorbed by getters. Getters are composed of a metal alloy that absorbs hydrogen to form a metal hydride. At some point the getters saturate, causing the receiver annulus to accumulate hydrogen. This buildup of hydrogen causes a significant decrease in collector field thermal efficiency and power plant electricity production (up to 15%).

Consequences

The issue of hydrogen generation and accumulation in parabolic trough plants is critical within the community of parabolic trough power plant owners and operators. Considering 5 GW of total capacity for the 80 operating plants operating worldwide, a 15% efficiency loss corresponds to 750 MW of lost power generating capacity. This loss equates to annual lost revenue of about $200 million from these power plants.

The NSO power plant started regular operation in 2008. In 2014, NSO began measuring elevated glass temperatures for some of their in-service receivers—an indication that hydrogen was accumulating in the receivers' annuli. In 2015, NSO and NREL began work to develop a hydrogen mitigation process that reduces dissolved hydrogen concentrations in the circulating HTF and permanently solves the problem of hydrogen buildup. Essentially all other commercial parabolic trough power plants worldwide began operating after 2008—this means that receiver conditions that were measured at the NSO plant in 2014 are indicators for what the rest of these

This report is available at no cost from the National Renewable Energy Laboratory at www.nrel.gov/publications.

power plants will see in coming years, and these plants will be faced with similar thermal efficiency and revenue losses.

Other mitigation solutions

The buildup of hydrogen in the vacuum annulus of the receivers was anticipated when the first parabolic trough power plants were designed and built by Luz. The original mitigation method was patented by Labaton et al. [6]. Their solution was to incorporate a palladium or palladium alloy membrane into the boundary between the receiver vacuum annulus and ambient air. Palladium and its alloys are exclusively permeable to hydrogen. The membrane could take the shape of a flat disc or thimble and provided a pathway for hydrogen to permeate from the vacuum annulus to ambient air. This method worked very well initially. However, with time the palladium membrane embrittled, lost strength, and failed. Hydrogen embrittlement occurs when a metal is exposed to hydrogen for extended periods. In addition to permeating, hydrogen dissolves into the metal and weakens metal bonds, causing the metal to lose strength. Hydrogen embrittlement can be avoided in palladium membranes if the membrane is kept above 300°C when it is exposed to hydrogen. The palladium membranes that were used in the original receivers were at elevated temperature when the receivers were on sun. During the evening, the receivers and membranes cooled down to ambient temperature while the palladium was still exposed to hydrogen, which caused the membranes to embrittle and fail.

More recently, we learned that palladium embrittlement is due to a palladium alpha to beta phase transition at 298°C [7]. Embrittlement occurs in the palladium beta phase, but not in the alpha phase. Alloying palladium (70%) with silver (30%) lowers the alpha to beta phase transition temperature to 0°C. Using this alloy would reduce the risk of embrittlement in solar field receivers but would not eliminate it because temperatures drop below 0°C regularly in the winter season. We use the palladium/silver alloy for our module membrane with an electric heater to ensure that the membrane does not drop below 150°C at any time.

The standard method for addressing hydrogen buildup is to incorporate getters into the receiver annulus. The getter material absorbs hydrogen and maintains hydrogen pressure to less than 0.01 mbar for about the first six operating years. After this time, the getters saturate and the receiver loses performance. Replacing compromised receivers every six years is a solution. However, a 70-MW power plant has 19,000 receivers in its collector field. Replacing these receivers is labor intensive and expensive. Each receiver is welded in place, so replacing requires cutting out the compromised receiver and welding in the new one. The cost to replace one receiver (labor and materials) is about $1,000, so replacing receivers in the entire solar field would cost about $19 million. In reality, not all receivers are compromised after six years, but a significant number of them are and replacing them is a serious financial burden, which must be paid by the plant owner and/or the receiver manufacturer. Furthermore, replacing receivers is not a permanent solution to the problem. Six years after the new receivers are installed, they need to be replaced again due to the next round of hydrogen buildup.

Another method that is being practiced by several power plants is to reduce the maximum operating temperature of the HTF a few degrees C by increasing the HTF flowrate in the collector field. The hydrogen generation rate due to HTF degradation is highly temperature dependent, so reducing the maximum operating temperature has a significant impact on hydrogen levels in the HTF. This practice has its greatest benefit during the summer months.

This report is available at no cost from the National Renewable Energy Laboratory at www.nrel.gov/publications.

Most recently, a mitigation method was developed that is based on the addition of a noble gas, argon, into the receiver annulus that has accumulated hydrogen [8, 9]. The gas acts to disrupt heat transfer due to hydrogen molecules in the annulus and significantly lowers heat loss. Argon must be injected into the receivers' annulus while they are in place on the collector assembly, which requires time and labor. This method has been used with success at NSO and ultimately may be a viable solution to the hydrogen issue.

3 Previous NREL Work Relating to a Hydrogen Mitigation Solution

Initial concept for hydrogen mitigation in parabolic trough power plants
Several years before the start of this TCF project, NREL identified and patented a mitigation concept that controls hydrogen levels by extracting hydrogen from the HTF in the expansion tanks [10]. The method consisted of extracting hydrogen from the headspace gas in the expansion tank at a prescribed rate. Reducing hydrogen in the headspace gas would reduce dissolved hydrogen in the circulating HTF. Initial modeling indicated that the method would work, but the specific method for hydrogen extraction and separation and its benefit to the solar field receivers had not been determined. The patent described an approach in which hydrogen is separated from the headspace gas using a proton exchange membrane fuel cell. This approach was not reduced to practice and eventually abandoned.

Previous collaboration between NREL and AE
Prior to the start of this TCF project, NREL and AE engaged in a 3-year collaborative effort [11] to identify, develop, and demonstrate on laboratory-scale a method to reduce and control hydrogen levels at parabolic trough power plants. Objectives were to (1) develop a sensor that measures hydrogen levels in the power plant expansion tanks, (2) perform experiments to determine the impact of reducing hydrogen levels on the performance of the collector field receivers, (3) develop a model that predicts receiver lifetime as a function of receiver location in the collector field and dissolved hydrogen concentration in the HTF, (4) develop power plant models that predict hydrogen levels in the circulating HTF as a function of hydrogen extraction rates from the expansion tanks, and (5) design and demonstrate a method to extract hydrogen from the expansion tanks at a prescribed rate.

During the first year, we identified, developed, and demonstrated a sensor that measured hydrogen partial pressure in the headspace gas of the power plant expansion tanks [12, 13]. We performed extended heat loss testing of an in-service receiver that was removed from the NSO collector field [14]. This testing showed that extended heating of the receiver at its nominal operating temperature caused hydrogen to reverse permeate out of the receiver annulus through the absorber. We developed a power plant model [15] to (1) estimate steady-state hydrogen levels in all power plant components and subsystems that contain circulating HTF, and (2) determine the hydrogen extraction rate from the expansion tanks that is needed to reduce collector field hydrogen and maintain receiver performance. We developed a mass transfer model [16] for the expansion tanks that estimated rates of hydrogen transfer across the HTF liquid/gas interface as a function of headspace gas hydrogen partial pressure.

During the second year, we focused our effort to identify designs for the sensor and separation process units that would be installed at the NSO power plant. We conceived an integrated

This report is available at no cost from the National Renewable Energy Laboratory at www.nrel.gov/publications.

process module that combined the hydrogen sensing and separating functions into a single unit. This advance greatly simplified the mitigation process design and installation. NREL conceived an integrated sensor/separator module and submitted a patent application for the module, which issued as a U.S. patent in 2020 [17]. We performed extensive modeling of the integrated module design to estimate its performance and to design laboratory experiments that would give us the information needed to proceed to the power plant installation design. We used our modeling results to design and fabricate a laboratory-scale integrated module and test system that was used to demonstrate both separating and sensor functions [18]. We designed and constructed experiments to validate the numerical results obtained during the first year that predicted hydrogen mass transfer rates across the HTF liquid/gas interface in the expansion tank [19].

During the third year, work transitioned from modeling and laboratory-scale experiments to design the on-site installation at AE's NSO power plant. In August 2018, NREL was awarded a TCF project to continue this effort at the NSO power plant. With this funding, NREL and AE intended to install a full-scale version of this mitigation technology at the NSO power plant.

4 TCF Project Technology Development Approach

Breaking down the problem into discrete steps

The goal of the first CRADA was to develop a process that would remove hydrogen from the power plant expansion tanks at a rate that would significantly reduce hydrogen in the solar field HTF and extend receiver lifetimes to match the 25-year operating lifetime of the power plant. As part of the first CRADA work plan, we developed a methodology that allowed us to break down the overall goal into a series of smaller goals or steps that could be defined and quantified to give us a clear understanding of what was needed to create a workable mitigation process design.

This methodology took the form of the three computational models that are shown in Figure 4. Our goal was to control hydrogen levels in the HTF that circulate through the collector field receivers, so the first step was to quantify receiver lifetime versus HTF hydrogen concentration in the receiver absorber. We needed to know what level of dissolved hydrogen in the HTF allowed the receivers to last the operating lifetime of the power plant. This receiver model allowed us to establish target levels for dissolved hydrogen in the HTF that flows through the receiver absorbers.

The second step was to quantify the distribution of HTF hydrogen within all power plant components that contain circulating HTF. These components include the solar field receivers, crossover piping, supply and return piping, the steam generator, and expansion tanks. Hydrogen levels are influenced by hydrogen generation, permeation, and transport within the plant process equipment and piping. This step allowed us to quantify the relationship between hydrogen levels at various locations within the power plant. Specifically, the model allowed us to determine the impact of lowering hydrogen levels in the expansion tanks on hydrogen levels in the collector field HTF.

This report is available at no cost from the National Renewable Energy Laboratory at www.nrel.gov/publications.

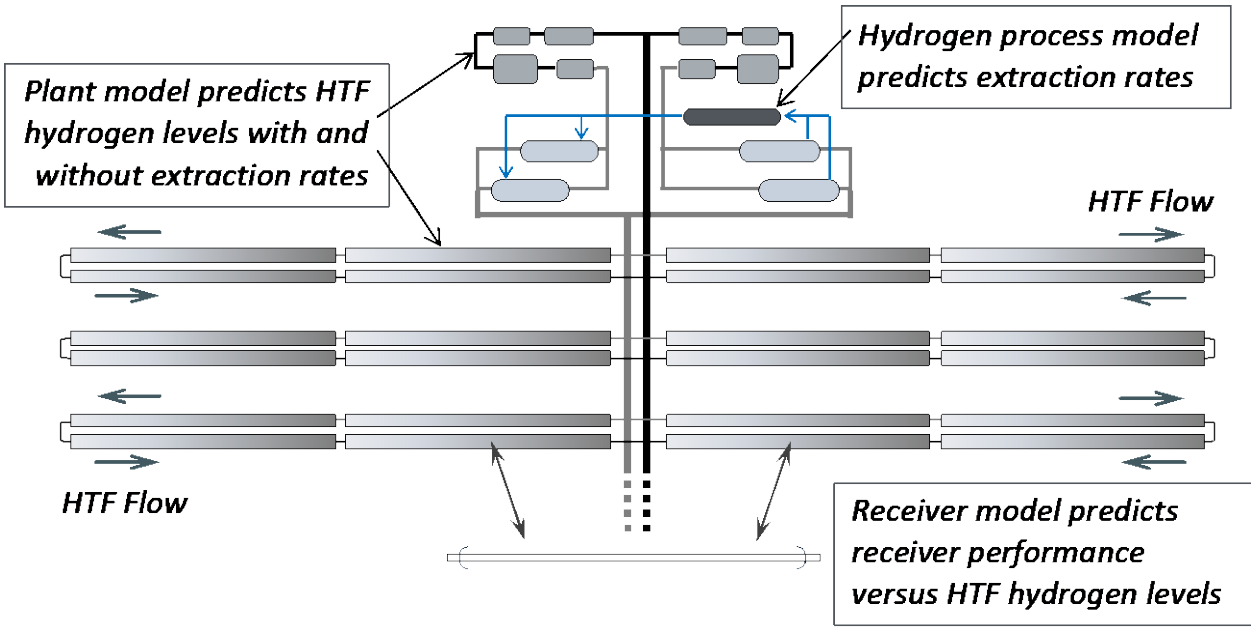

Figure 4. Steps to model and determine process rates

We used these two models to (1) determine the performance of collector field receivers versus their HTF hydrogen levels, and (2) determine the effect of reducing expansion tank hydrogen on collector field HTF hydrogen levels. With these models, we could generate specifications for the expansion tanks in terms of (1) their target levels of dissolved HTF hydrogen, (2) the corresponding hydrogen partial pressure in the headspace gas, and (3) the rate at which the mitigation process needs to extract hydrogen from the expansion tanks to control levels in the collector field HTF. We used these specifications for the expansion tank as inputs to the model that predicts hydrogen extraction rates for a given extraction process design. These three models together were used in the first CRADA to develop a process design that would reduce HTF hydrogen to target levels in the NSO solar field receivers.

For the TCF project, we used this same combination of models to guide the hydrogen extraction process design and installation at the NSO power plant. The receiver lifetime and process design models were essentially the same as those used in the first CRADA. For the TCF project, we developed a new dynamic power plant model that provided time-resolved hydrogen concentrations for locations in the NSO plant. The dynamic plant model predicted hydrogen levels with hourly resolution for representative days for 12 months of the operating year. This model provided a much clearer picture of hydrogen levels within the power plant as they vary by hour of the day and month of the year. This information was used to better predict extraction process performance and receiver lifetimes using the process performance and receiver lifetime models.

This report is available at no cost from the National Renewable Energy Laboratory at www.nrel.gov/publications.

5 TCF Project Tasks and Results

Task summary and scope

The original four tasks for this TCF project were (1) test-scale design and installation, (2) test-scale testing, (3) full-scale design and installation, and (4) full-scale testing. As NREL and AE progressed with specifying the test-scale process piping, equipment, sensors, and controls, AE realized that the time, cost, and effort needed just for the test-scale installation was all they could afford for the whole project scope. To address this issue, AE proposed to proceed with the test- and full-scale designs and installations as parallel efforts.

To stay within the limits of AE's available resources, we went directly to the full-scale design for the KOP, process piping, separation module, control valves, sensors, signal and power wiring, and programmable logic controller (PLC). We decided to stay with the test-scale specifications for the headspace gas blower and two vacuum pumps to keep equipment costs within reason. With this approach, AE was able to pay for and complete a process installation that would still meet their hydrogen reduction targets for the NSO solar field.

If the installed process did not meet their long-term performance targets, AE had the options to (1) purchase and install two higher-performance turbopumps that pump in series with the two existing vacuum pumps, (2) purchase and install a headspace gas blower with higher volumetric pumping capacity, and (3) install a second separation module. NSO installed pipe flanges that allow a second module to be installed in series or in parallel with the first module.

The COVID-19 pandemic caused many months of delay for the process commissioning. Travel restrictions during 2020 and the first months of 2021 prevented NREL and NSO from completing process startup and commissioning according to the original schedule. The pandemic delayed project completion by 15 months. NREL used this time to develop a dynamic power plant model that has much greater resolution with respect to predicting (1) HTF dissolved hydrogen concentrations, (2) hydrogen extraction process performance, and (3) long-term receiver lifetimes and solar field performance. One positive result is that the dynamic model predicts that the process that was installed at NSO could still meet NSO performance targets for extending solar field receiver lifetimes.

As a result of these circumstances, the work and accomplishments that are reported next are for (1) process installation and (2) process performance testing—knowing that the process that was installed had some of the design elements from both the test-scale and full-scale designs. The goal was the same—installation of a mitigation process at NSO that meets NSO's performance targets in terms of hydrogen reduction and solar field performance. All milestones remained the same as originally written.

Process installation—NSO headspace gas temperatures and pressures

NREL used 2017 HTF temperature and pressure operating data that were provided by NSO to develop headspace gas physical property (molar mass, density, specific heat capacity, viscosity, thermal conductivity) mappings for the most frequent and most extreme HTF operating conditions. These properties were used in standard turbulent pipe flow momentum, heat, and mass transfer models to calculate the range of pressure drops in supply, platform, and return piping, and hydrogen transfer rates in the separation module. Results were used to (1) estimate

This report is available at no cost from the National Renewable Energy Laboratory at www.nrel.gov/publications.

the pumping power and volumetric capacity for the headspace gas blower and (2) estimate the thermal power needed for the piping heat trace and for the membrane rod heater that maintains the membrane temperature during operation.

Figure 5 maps the occurrence of temperature and pressure for the headspace gas. The hourly data showed a wide range of expansion tank headspace gas temperatures and pressures. The three most common conditions are circled in purple (50 psig and 210°C; 65 psig and 245°C; 100 psig and 285°C) and four extreme conditions are circled in red (14 psig and 175°C; 35 psig and 125°C; 105 psig and 290°C; 130 psig and 285°C). Thermal and mechanical power requirements for the headspace gas and electric heaters were calculated for these seven conditions.

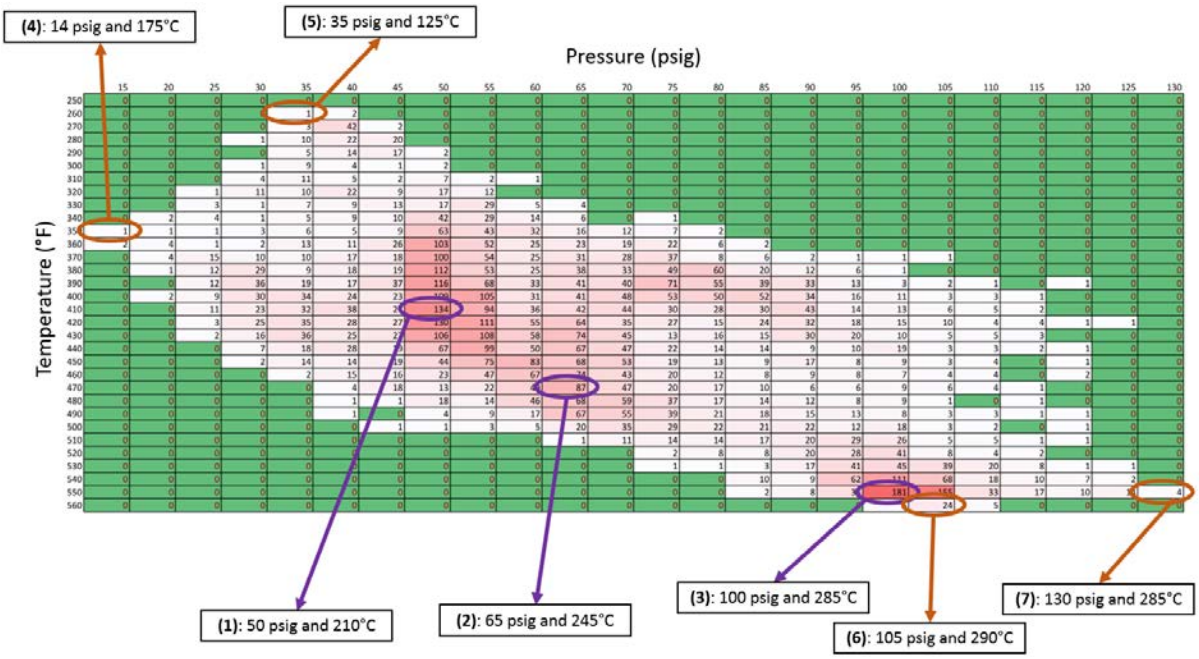

Figure 5. Hourly distribution of temperature in °F and pressure in psig for the NSO expansion tank headspace gas in 2017. Numbers in each temperature/pressure condition are the total hours that condition occurred in 2017.

Process installation—piping layout

Figure 6 shows the existing piping that was accessed for the mitigation process installation. Plant nitrogen is supplied via existing piping to the two south and two north expansion tanks. Ullage piping that is above the four tanks vents headspace gas to the power plant catalytic oxidizer. These two systems purge and vent hydrogen, moisture, and other products of HTF from the expansion tanks to maintain proper pressure and composition of the headspace gas in the tanks.

To access the expansion tank headspace gas, NSO installed the supply, return, and process piping shown in Figure 6. NSO installed the isolation valves to isolate gas flow between the expansion tanks and the process. Major process equipment included the KOP, separation module, headspace gas blower, flow control valves, permeate valve, two vacuum pumps, and catalytic oxidizer.

This report is available at no cost from the National Renewable Energy Laboratory at www.nrel.gov/publications.

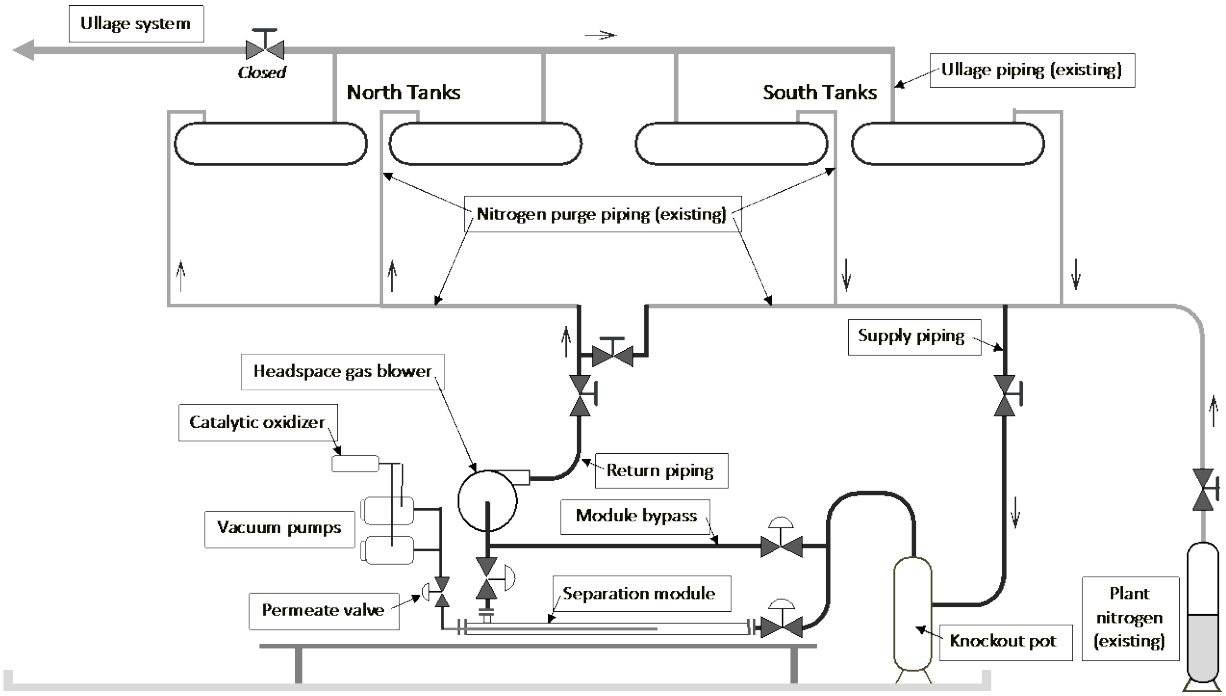

Figure 6. Existing and new piping for the test-scale process layout

NSO installed the piping and major equipment pieces onto the process platform that is shown in Figure 7. Figure 7 shows the KOP located adjacent to the platform and the separation module and two vacuum pumps located on the platform. The piping sections include the straight piping section that holds the vortex flowmeter. Figure 7 shows the location of the headspace gas blower and ½" tubing manifold.

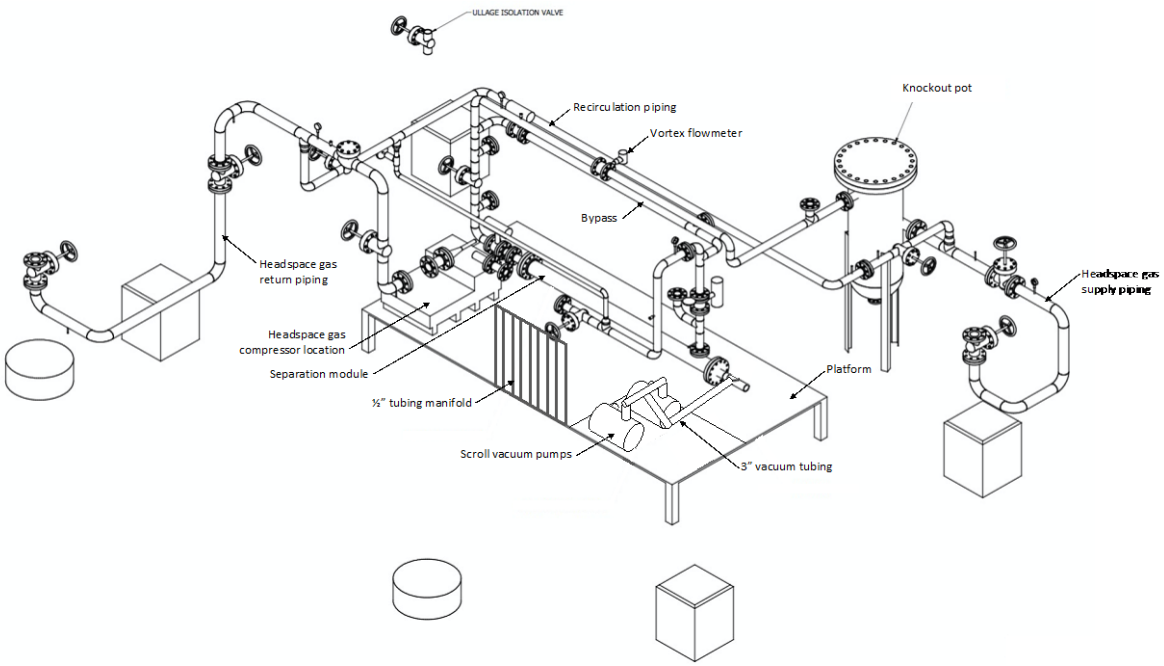

Figure 7. 3D assembled piping and equipment layout on the process platform

This report is available at no cost from the National Renewable Energy Laboratory at www.nrel.gov/publications.

The piping was divided into several sections and welded as spool pieces. Each spool piece had its own dimensioned 3D drawing to ensure that the spool pieces, KOP, separation module, and blower fit precisely together when assembled. Figure 7 shows locations for process piping for the module inlet, module outlet, and module bypass. The vortex flowmeter mounted into a straight piping section, which ensured fully developed flow of the headspace gas on each side of the vortex meter to make an accurate flow measurement. Figure 7 shows the 3" vacuum tubing that connects the permeate volume outlet to the two scroll vacuum pumps. The two vacuum pumps had isolation valves at their inlets and connected to the permeate volume outlet with 3" vacuum tubing.

Process installation—piping insulation and heat trace
NSO applied insulation and heat trace to the supply, return, platform pipes, and separation module and the KOP for several reasons:

1. Limit heat losses from the process gas to the environment
2. Limit the amount of HTF condensation accumulating in the KOP
3. Assist with maintaining a sufficiently high palladium membrane temperature (>250°C) to prevent membrane embrittlement
4. Assist during the module startup phase when all piping and H_2 removal equipment is brought to the operating temperature.

Figure 8 shows the layout and diameters of the process piping and equipment. NREL developed a heat transfer model in MATLAB [20] to estimate heat losses occurring in piping, module, and KOP, and estimate the required insulation thickness, and heat trace length and power for each component. The model considered HTF condensation in the piping with corresponding heat of condensation/evaporation, and at the outer surface—both convective heat transfer using Nusselt correlations and radiative heat transfer—assuming emissivity of 0.7. The insulation thermal conductivity was set to 0.04 W/(m-K). We assumed a worst-case scenario with 10 m/s wind speed, 300°C HSG temperature, 100 psig HSG pressure, 200 ACFM flow rate, and ambient temperature at -18°C (0°F). The module inside wall temperature was set to 320°C.

This report is available at no cost from the National Renewable Energy Laboratory at www.nrel.gov/publications.

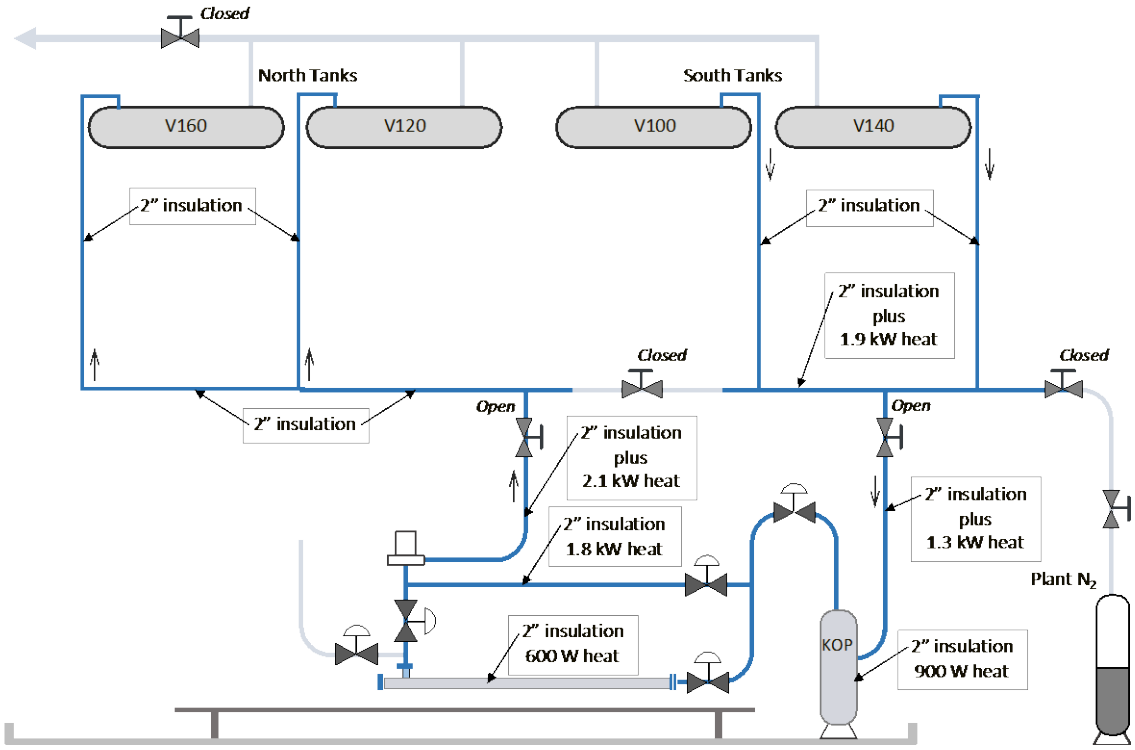

Figure 8. Insulation thickness and heat trace power for piping, module, and KOP—insulated piping is shown in blue

Results for the heat transfer calculations indicated that heat losses and HTF condensation were limited by applying 2" of insulation to all components (module, KOP, and supply, return, and platform piping) and 600 W to 2.1 kW of heat trace to all components except the 2" vertical supply pipes, and 2" and 3" vertical return pipes that are shown in Figure 8. Heat trace and insulation were supplied and installed by a local Nevada vendor.

Table 1 summarizes the results for the most extreme conditions taken from Figure 5. For -18°C (0°F), the KOP fills up in 20 hours; at 0°C in 30 hours. For ambient temperatures above 10°C, the HTF fill rate in the KOP is negligible.

This report is available at no cost from the National Renewable Energy Laboratory at www.nrel.gov/publications.

Table 1. Summary of heat transfer calculation results for worst-case scenario (10 m/s wind velocity, -18°C ambient temperature, 300°C HSG temperature, 100 psig HSG pressure, 200 ACFM flow rate)

Knockout pot (results without heat trace)					
Insulation Thickness (inch)	Ambient Temperature (°C)	Radiative Heat Losses (kW)	Convective Heat Losses (kW)	Total Heat Losses (kW)	Surface Temperature (°C)
2	-18	0.08	1.04	1.12	-11.8
Platform piping (30 ft length; results without heat trace)					
Insulation Thickness (inch)	Ambient Temperature (°C)	Heat Losses (W/ft)		Total Heat Losses (kW)	Surface Temperature (°C)
2	-18	31.6		0.95	-14.7
Membrane module (results without heat trace and for 320°C inside module wall temperature)					
Insulation Thickness (inch)	Ambient Temperature (°C)	Heat Losses (W/ft)		Total Heat Losses (kW)	Surface Temperature (°C)
2	-18	51.4		0.51	-13.8
Supply piping (with 3 × 20 W/ft heat trace at 3" and 4" pipe sections)					
Insulation Thickness (inch)	Ambient Temperature (°C)	Temperature drop (°C)	Heat lost to environment (kW)	Net heat losses including heat trace and condensation (kW)	Time to fill KOP (hours)
2	-18	0.12	3.9	0.2	21
Return piping (with 3 × 20 W/ft heat trace at 4" pipe section)					
Insulation Thickness (inch)	Ambient Temperature (°C)	Temperature drop (°C)	Heat lost to environment (kW)	Net heat losses including heat trace and condensation (kW)	HTF condensation (GPH)
2	-18	4.0	7.9	5.8	0

NSO installed heat trace cables on various piping segments of the hydrogen mitigation system to assist with maintaining elevated HTF temperature to limit fluid condensation and achieve high membrane performance. Specifically, five heat trace circuits were installed, labeled heat trace #1 through #5. They were located on the headspace gas supply piping, piping from the KOP to the module, the bypass line, the separation module itself, and the piping from the module to the compressor (Figure 9).

This report is available at no cost from the National Renewable Energy Laboratory at www.nrel.gov/publications.

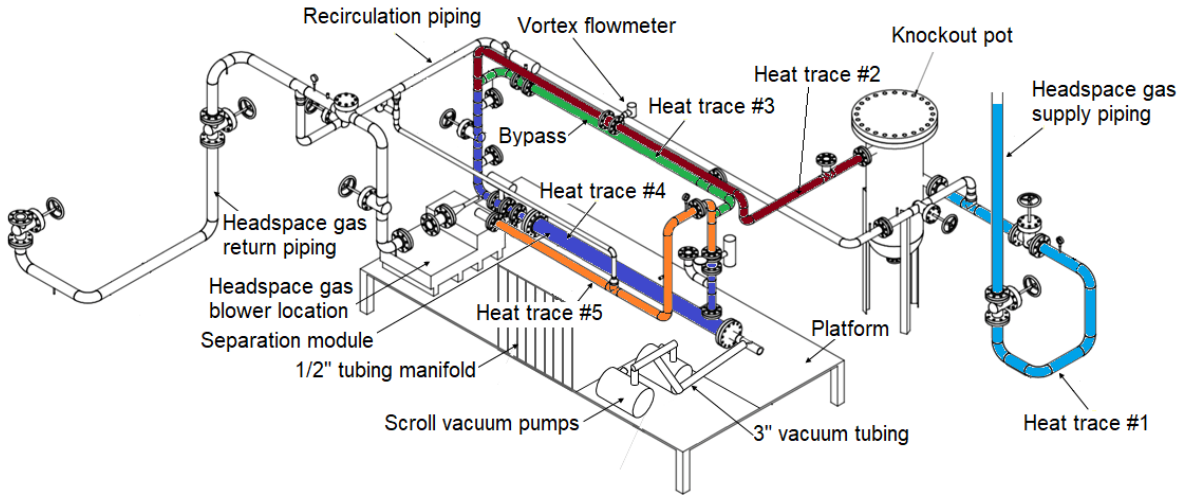

Figure 9. Schematic diagram of mitigation process with five heat trace circuits color-coded and labeled

Heat trace cable lengths were between 5 m and 10 m, and their heating output was between 1.0 kW and 2.3 kW. NSO installed heat trace directly onto the piping underneath 3" of insulation. Each circuit had its own temperature measurement using a Type K thermocouple to allow for individual heat trace temperature control. NREL connected the five heat trace circuits to the PLC—both incoming thermocouple signals and the outgoing control signals to the relays for the circuits. For safety reasons, two relays were installed for each circuit—one on each heater lead NREL programmed the PLC to control each heat trace output to maintain a user-defined heat trace set point temperature. The heat trace circuits, thermocouples, heating output and PLC control were tested successfully up to a setpoint of 250°C.

Process installation—separation module and membrane assembly

Figure 10 shows the membrane assembly and insert components. The membrane assembly consisted of a 3.5" OD stainless steel tube with 1/8" perforations that allow hydrogen to transfer into the permeate volume. The tube provided support to the membrane that is 0.005" thick and needed to withstand 120 psi pressure drop across it from outside to inside. Other components were the 3" Sch 40 flanged insert that has a welded 3" side pipe with a flange that connects to the permeate valve and vacuum tubing. The end cap seals the free end of the insert. The insert included a 5-kW electric cartridge rod heater that maintained the temperature of the membrane. The insert was located inside the separation module and sealed to a flange on one end of the module with the flange that is welded to the 3" Sch 40 pipe.

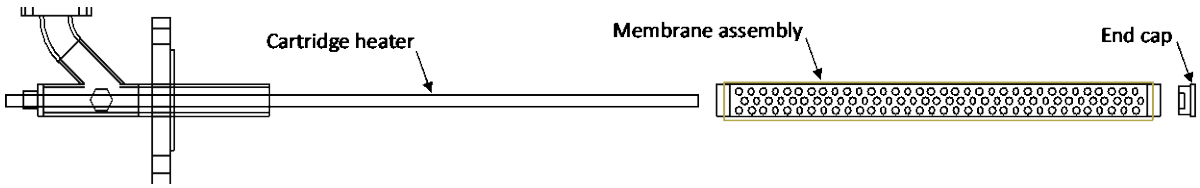

Figure 10. Membrane insert components including membrane assembly

This report is available at no cost from the National Renewable Energy Laboratory at www.nrel.gov/publications.

Proper membrane function required that only hydrogen transfer to the permeate volume from the headspace gas, so the membrane assembly and membrane insert needed to seal well. Figure 11 shows the palladium membrane after it was brazed axially and at both ends to seal the assembly. After brazing, the assembly was pressurized and checked for leaks. We repeated this process several times to eliminate leaks and ensure that the membrane assembly sealed properly.

The next steps in the assembly process were to weld the end cap to the membrane assembly and the assembly to the insert, as shown in Figure 11. The insert weld needed to have good alignment between the membrane assembly and insert piping, so the membrane was centered in the separation module. Significant misalignment would interrupt the turbulent headspace gas flow profile in the module annulus.

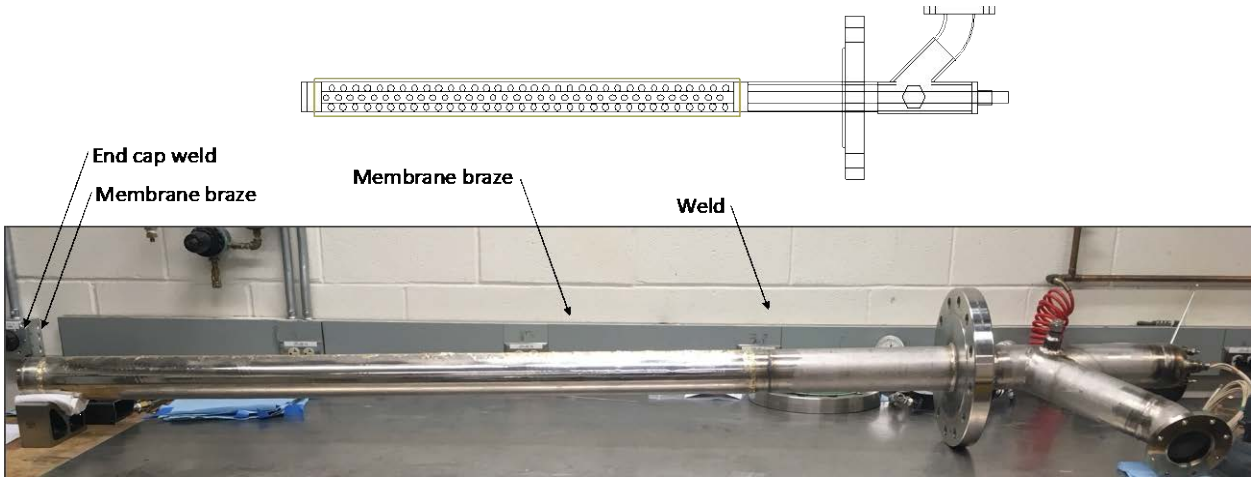

Figure 11. Welded insert and membrane components

NREL performed a series of tests on the separation module and membrane before shipping the assembly to NSO. After the palladium membrane was brazed together and welded to the membrane insert, NREL checked for leaks by pressurizing the permeate volume of the membrane assembly to 7 psig and checking all braze and weld joints by applying a soap solution. Next, NREL evacuated the permeate volume of the membrane assembly and used a vacuum transmitter to measure low pressure (Figure 12).

This report is available at no cost from the National Renewable Energy Laboratory at www.nrel.gov/publications.

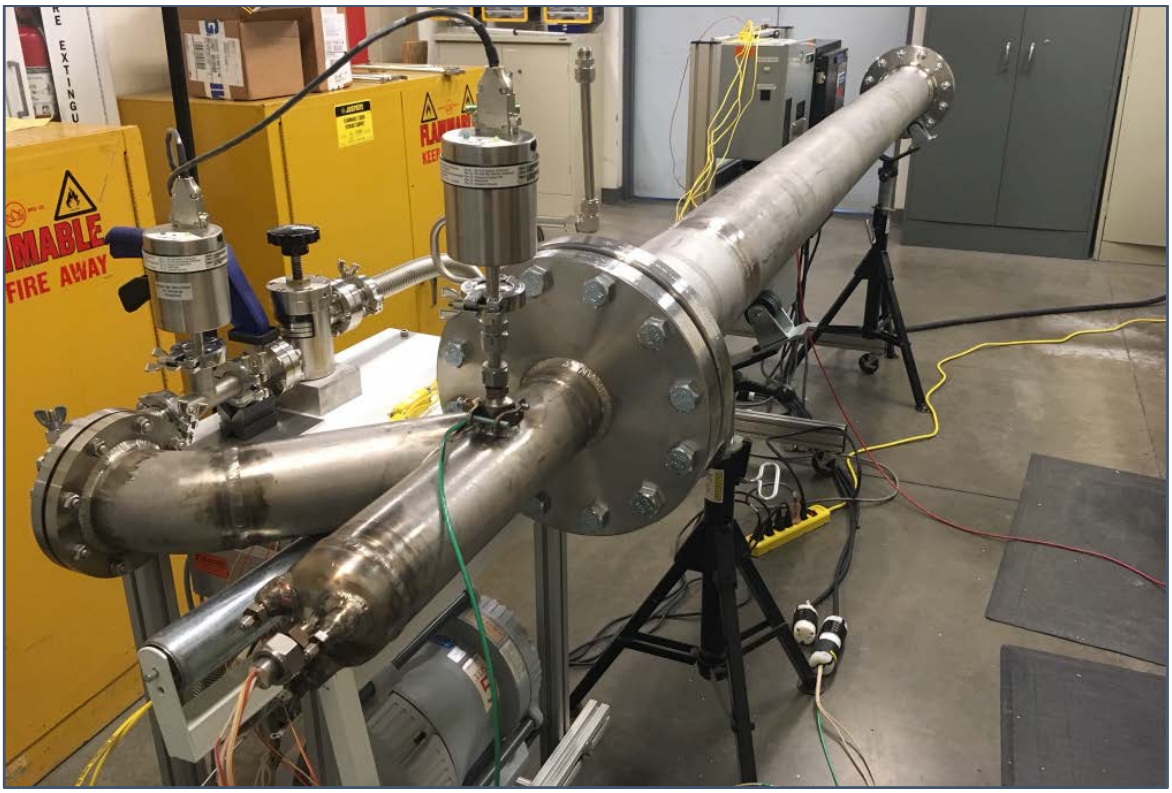

Figure 12. Separation module and palladium membrane testing at NREL

Scroll and turbo pumps were used in series to reduce volume pressure to 0.0001 mbar at ambient temperature. We closed the valve that isolates the permeate volume from the vacuum pumps. Any significant leaks or surface degassing causes the pressure in the volume to increase. The measured pressure increase was 0.00015 mbar/minute. This increase caused less than 0.1% error in the hydrogen partial pressure measurement during operation.

Figure 12 shows the electrical leads for the rod heater in the lower left of the photo. A vacuum gage (center) measured low pressure in the permeate volume and a second gage (left) measured pressure in the separation module. This pressure is the applied pressure to the outer surface of the membrane. We purged the separation module with nitrogen to remove any air and evacuated the permeate volume that is enclosed by the membrane. Using the rod heater, we heated the membrane to 330°C—its maximum membrane operating temperature. When the temperature reached steady state, we increased the module pressure to 200 psig. The maximum pressure the membrane will ever see is 160 psig. The pressure drop across the membrane was 212 psi from outside to inside with the membrane temperature at 330°C. We held these conditions for 15 minutes and then reduced the pressure to 140 psig—the maximum operating pressure. We held these conditions for one hour and tested for leaks by closing the isolation valve shown in Figure 12. The detected leakage rate did not increase compared to the rate that was measured at ambient temperature and pressure. With these tests, we were confident that the membrane would tolerate the temperature and pressure of the headspace gas as it flows through the module.

This report is available at no cost from the National Renewable Energy Laboratory at www.nrel.gov/publications.

Process installation—installed separation module and membrane assembly
Figure 13 shows the installed separation module after insulation and heat trace was added. The two permeate volume vacuum pumps are seen behind the separation module. Above and behind the module is insulated piping, including heat trace that goes from the module to the headspace gas compressor.

Figure 13. Heat trace and insulation added to separation module at NSO

Process installation—knockout pot with vortex breaker, level sensor and control
NREL and NSO designed the KOP shown in Figure 14. The KOP had an inlet flanged port (b) that was mounted tangential to the outside surface of the KOP. Headspace gas entered the inlet and swirls in the lower section of the KOP, causing liquid droplets to separate from the gas. The headspace moved up through the demister to remove liquid droplets down to 10 microns before existing the KOP through the outlet flanged port (a) at the top of the KOP. Separated liquid drained through a port at the bottom of the pot.

NREL and NSO specified a vortex breaker and magnetic level indicator (MLI) and added those to the KOP design shown in Figure 14. Figure 15 shows the vortex breaker design and location, which were based on standard sizing guidelines for design of liquid storage vessels. The vortex breaker is a horizontal disc that is located just above the drain at the bottom of the KOP. When the pot's liquid is draining, the vortex breaker prevents the formation of vortices just above the drain and prevents suction of gas down through the liquid and into the drain. Nick's Welding, Inc. added the breaker to the KOP as shown in Figure 15.

This report is available at no cost from the National Renewable Energy Laboratory at www.nrel.gov/publications.

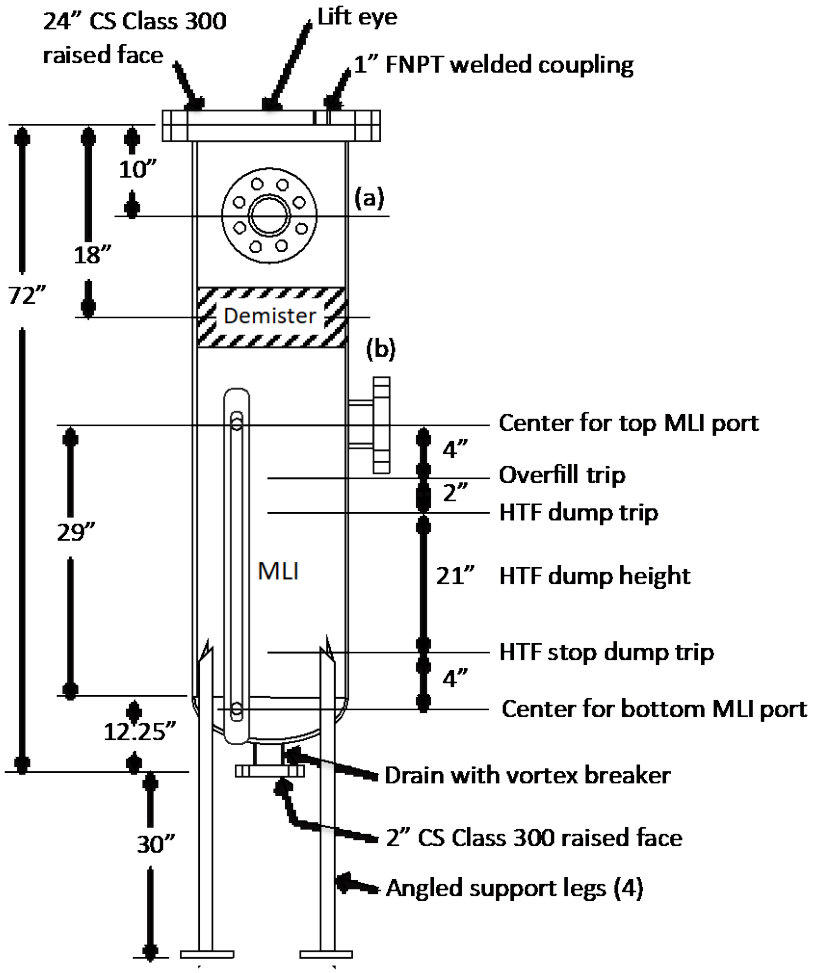

Figure 14. KOP showing locations of vortex breaker and MLI

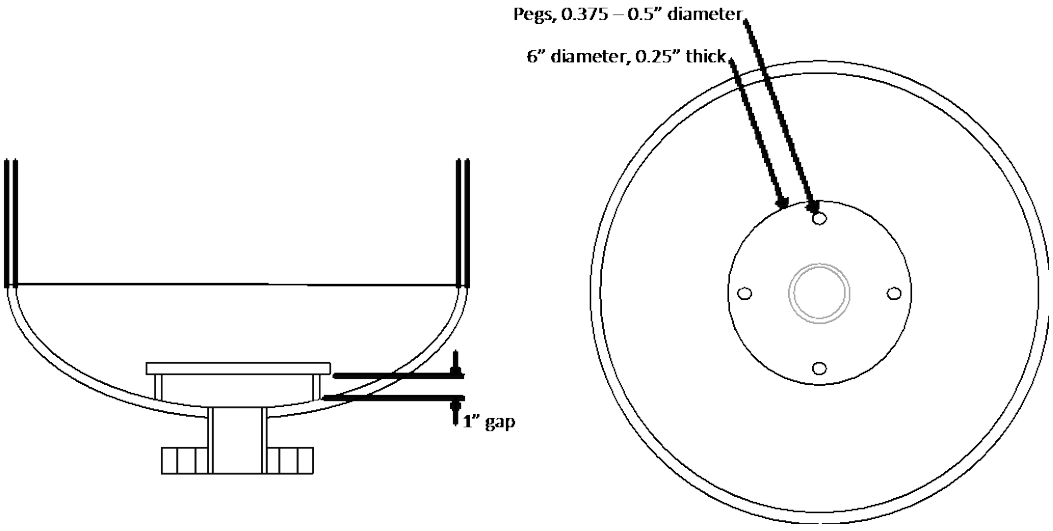

Figure 15. Design and location of vortex breaker in bottom of KOP

This report is available at no cost from the National Renewable Energy Laboratory at www.nrel.gov/publications.

The MLI was located on the side wall of the KOP, as shown in Figure 14 and Figure 16. The main chamber of this device holds HTF liquid that equalizes level with the HTF liquid in the KOP. The main chamber has a float that has a magnet. The magnet flips fixed magnets on the visual indicator to show the liquid level. The chamber and connections are stainless steel and can tolerate the temperature and pressure of the liquid HTF in the KOP. Isolation valves were added to the connections to allow for disconnecting and/or replacing the MLI.

The MLI assembly included three level switches that are tripped by the floating magnet when the magnet is at the same height as the switch. The top switch indicates an overfill condition and sends a signal to the PLC to shut down the process. The middle switch sends a signal to the PLC to open the drain valve and dump HTF liquid. Dumping continues until the HTF level and floating magnet reach the bottom level switch, which then sends a signal to the PLC to close the drain valve. The MLI provided a visual measure of liquid height to personnel, who are operating the process, and the level switches maintain the amount of liquid in the KOP between high and low limits.

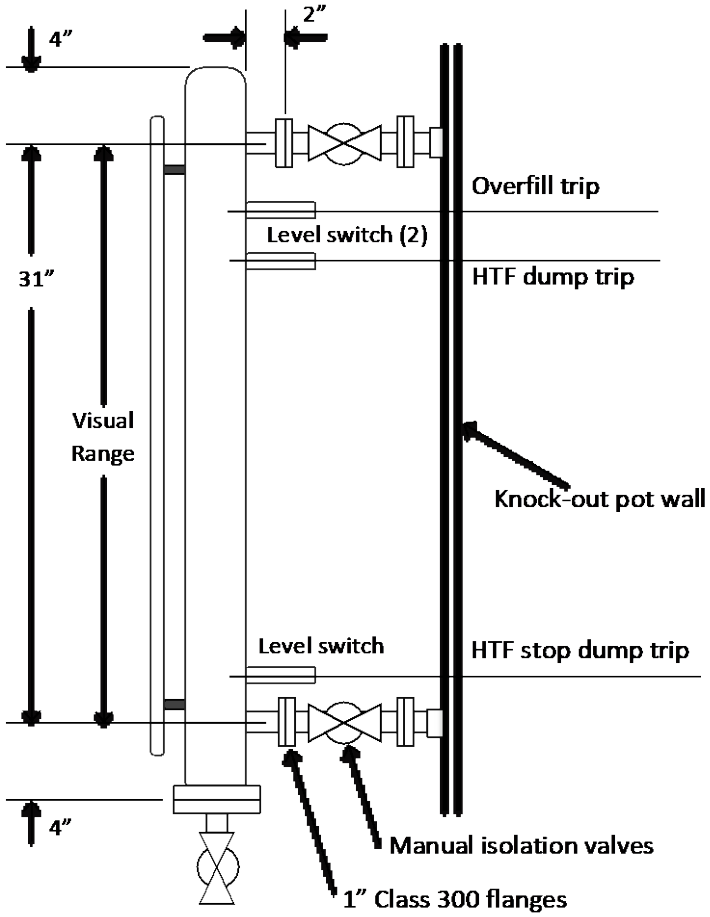

Figure 16. Design and location of MLI with level switches

This report is available at no cost from the National Renewable Energy Laboratory at www.nrel.gov/publications.

Nick's Welding fabricated the KOP with top cover flange, the vortex breaker, and the flange connections for the MLI. Nick's welding performed hydrostatic testing of the vessel and all flanges to certify it as a U-stamped pressure vessel according to ASME pressure vessel codes.

Process installation—headspace gas compressor selection
NSO and NREL identified a compressor that met the requirements of the test-scale process that was supplied by Schaeff of Houston. This compressor was Class 1 Div 2 certified and did not need any additional housing to make it meet the explosion-proof requirements that applied to the process installation. The variable frequency drive (VFD) that provided power to the compressor was located in an isolated, temperature-controlled room that was not part of the Class 1 Div 2 area, and so did not need any additional housing. NREL and NSO specified compressor power versus process gas flowrate for the compressor in the range of 150 ACFM to 200 ACFM. Figure 17 shows compressor power versus volumetric flowrate for representative process gas conditions.

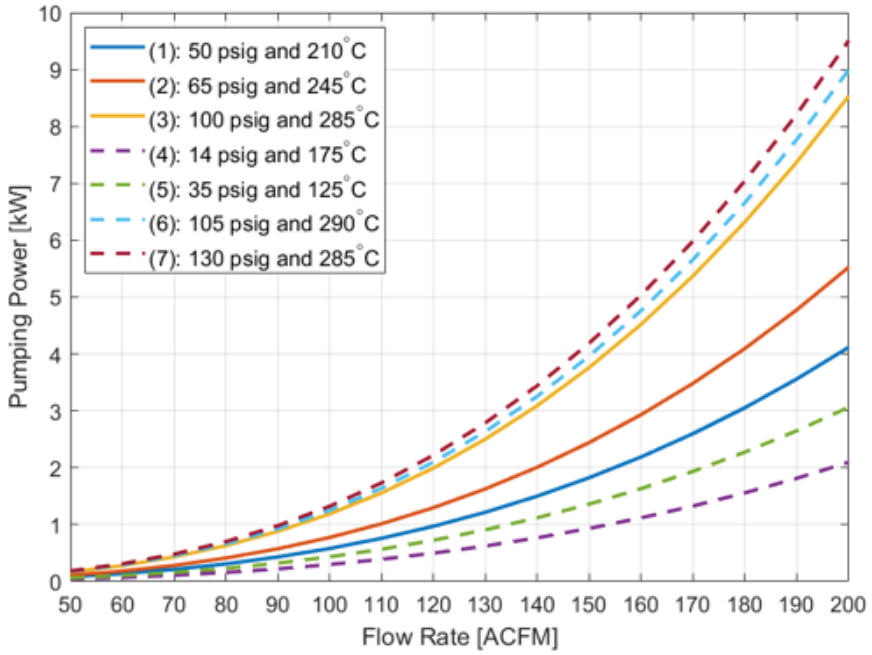

Figure 17. Compressor power versus process gas volumetric flowrate—power requirement due to flowing process gas through piping and valves

With the flowrate range from 150 ACFM to 200 ACFM, this compressor generated the process gas flowrate needed for the process using the supply, platform, and return piping that was installed for the test-scale process. NSO and NREL will be able to transition from the test-scale to the full-scale process without needing to change the compressor or any of the process gas piping. This benefit saved significant time and cost, when installing the full-scale process.

Process installation—permeate volume vacuum pump selection
NREL considered several options for the vacuum pumps that evacuate the permeate volume when hydrogen is extracted from the headspace gas. The best-suited pump for this application needed to evacuate the permeate volume to low pressure and have high volumetric pumping

This report is available at no cost from the National Renewable Energy Laboratory at www.nrel.gov/publications.

speeds. Vacuum pumps are generally designed to have one of these two features, but not both. The reason for these requirements is that the rate at which hydrogen is removed from the permeate volume is fixed by the power plant model. For the test-scale installation, we set the target removal rate to be $4.5X10^{-4}$ mole/s.

We wanted the permeate hydrogen concentration to be as low as possible to promote hydrogen transfer across the membrane. The removal rate is the product of the hydrogen concentration (mole/m^3) and the volumetric flowrate (m^3/s), so as the concentration decreases, the volumetric flowrate must increase to keep the removal rate constant. To meet this condition, the pump needed to pump down to low pressure while maintaining a high pumping speed.

We surveyed many candidates for this application. The best options in terms of performance were high-capacity turbopumps. These pumps are capable of pumping down to very low pressures (0.1 μbar), while maintaining high pumping speeds. The issues with these pumps are (1) they are very large and heavy, (2) they are expensive, and (3) they require significant maintenance. Several other pumps had similar characteristics, including rotating lobe displacement pumps. These pumps also were quite expensive and power intensive.

We selected a positive displacement scroll pump that has good pumping speed (8 L/s) at reasonably low pressure (0.7 mbar). To meet our target removal rate, we calculated that hydrogen concentration at 0.7 mbar pressure is $2.8X10^{-5}$ mole/L, so our pump speed needed to be 16 L/s to achieve the removal rate. To meet this pump speed, we elected to purchase and install two scroll vacuum pumps in parallel with each one pumping at 8 L/s. With this hydrogen removal rate and permeate pressure, our separation module transport model predicted that the headspace gas hydrogen partial pressure should decrease to 3 mbar, which is 3.3X less than the partial pressure when there is no hydrogen removal (10 mbar). NSO purchased two Edwards Vacuum scroll pumps model XDS46i to remove hydrogen from the permeate volume. The pumps were delivered to NREL for vacuum tube fitting and initial testing. NREL completed specification and inspection of the two vacuum pumps and accessories that along with the vacuum pumps, form the vacuum system that extracted hydrogen from the separation module. The two scroll pumps were inspected by the NREL electrician to verify that they meet the Class 1 Div 2 certification.

NREL specified two water-cooled radiators that maintain the cooling air temperature to less than 32°C, which was needed to keep the pumps from overheating during summertime operation. The vacuum system was sized originally to allow the two vacuum pumps to remove hydrogen from the permeate volume at a rate of about $5X10^{-4}$ moles/s, while maintaining the permeate volume hydrogen pressure at 0.7 mbar. These conditions were needed to reduce hydrogen partial pressure in the headspace gas from about 10 mbar, when the process is not operating down to 2.5 mbar, when the process is extracting hydrogen from the headspace gas. All flanges and tubing were either the ISO80 or KF50 standards.

Process installation—catalytic oxidizer

Based on data obtained from experiments with an initial prototype design, NREL designed a catalytic oxidizer that would achieve full conversion of hydrogen without active (electric) heating at full-scale hydrogen removal conditions (4 g H_2/hr). This design (Figure 18) used four Tanaka Platinum Honeycomb catalysts in series and had a coaxial tubing configuration for

This report is available at no cost from the National Renewable Energy Laboratory at www.nrel.gov/publications.

preheating of the inlet gas stream with heat generated by the hydrogen oxidation reaction. This design featured a pre-heat zone in which the hydrogen/air mixture is heated to 70°C using the heat of oxidation before entering the catalyst. This design required no electrical preheating, which would have required Class 1 Div 2 heaters when implemented at the process site at NSO.

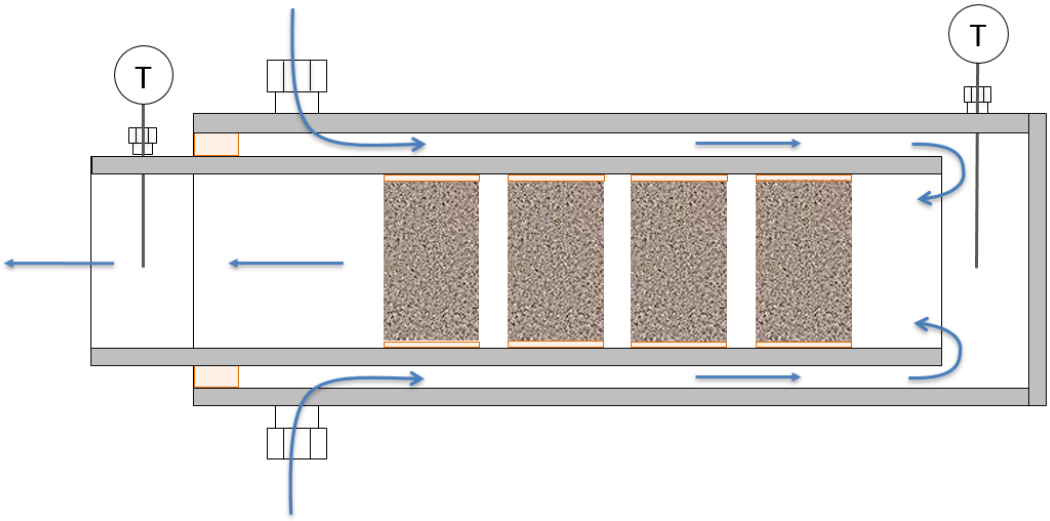

Figure 18. Catalytic oxidizer with four catalysts in series and inlet gas preheating

Figure 18 shows the hydrogen/air flow pattern through the catalytic oxidizer assembly and illustrates how the inlet gas is pre-heated in the annulus by the four catalyst discs. This feature increases the gas temperature up to 40 to 50°C before it enters the first catalyst and ensures complete hydrogen conversion to water vapor. Figure 19 shows ½" tubing that supplied the hydrogen/air mixture to the assembly. Converted gas exits the assembly through the circular outlet on its right end.

Figure 19. Catalytic oxidizer during testing at NREL

Thermocouples were used to monitor operation and estimate performance. We calculated annulus heat transfer and pressure drops in MATLAB that indicated an optimal annulus gap of about 1/16 inch. The heat transfer calculations showed that the gas temperature after preheating reaches about 75°C. Experiments showed that with an inlet temperature of 75°C and 4.0 g H_2/hr flow rate, two catalysts generated a temperature rise up to 120°C but did not achieve full conversion. However, the 120°C inlet temperature was enough to achieve full conversion with

This report is available at no cost from the National Renewable Energy Laboratory at www.nrel.gov/publications.

two additional catalysts. Hence, we used a total of four catalysts for the final design. During testing we measured temperatures at the assembly gas inlet and outlet, and measured hydrogen concentration at the outlet using a combustion gas detector. Table 2 summarizes the total gas flow rate and hydrogen concentration for 11 tests.

Table 2. Summary of hydrogen flow test conditions and resulting hydrogen conversion

Exp. #	Dry air flow rate (CFM)	10% H_2 flow rate (CFM)	Total flow rate (CFM)	H_2 flow rate (g/hour)	H_2 conc. (%)	Summary
1	0.75	0.500	1.25	5.91	4.0	0 ppm hydrogen detected
2	3.50	0.500	4.00	5.91	1.3	> 0 ppm hydrogen
3	2.50	0.500	3.00	5.91	1.7	0 ppm hydrogen detected
4	3.00	0.500	3.50	5.91	1.4	0 ppm hydrogen detected
5	3.17	0.330	3.50	3.90	0.9	> 0 ppm hydrogen
6	2.67	0.330	3.00	3.90	1.1	> 0 ppm hydrogen
7	2.17	0.330	2.50	3.90	1.3	> 0 ppm hydrogen
8	1.67	0.330	***2.00***	3.90	1.7	***0 ppm hydrogen detected***
9	1.50	0.500	***2.00***	5.91	2.5	***0 ppm hydrogen detected***
10	1.75	0.250	***2.00***	2.96	1.3	***0 ppm hydrogen detected***
11	1.58	0.420	***2.00***	4.97	2.1	***0 ppm hydrogen detected***

From these results and the measured outlet temperatures, we concluded:

1. Experiments that were run at >2 CFM total flow rate detected hydrogen at the outlet for some hydrogen flow rates.
2. Experiments run at 2 CFM total flow rate detected no hydrogen at the outlet for hydrogen flow rates from 3 g/hour to 6 g/hour.

Because the range of hydrogen flow rates for all test-scale and full-scale operating conditions is 3–6 g/hour, we can ensure complete hydrogen conversion if we keep the total flowrate at 2 CFM. Our testing with this design established the operating temperatures and gas flowrates that were used when the catalytic oxidizer was installed in the process at NSO.

After testing was completed at NREL, the catalytic oxidizer was shipped to NSO and installed at the mounting location just above the two vacuum pumps. We used ½" tubing to connect the outlet vents from the two vacuum pumps to the inlet of the catalytic oxidizer.

Process installation—½" tubing manifold
Figure 20 shows the ½" process tubing layout. The layout includes solenoid, isolation, safety relief, and check valves, along with pressure regulators, flowmeters, and pressure transmitters. The tubing sections are listed to the left of the drawing and are (1) plant air and vacuum pump outlets for sending hydrogen to the catalytic oxidizer, (2) separation module discharge to the ullage system, (3) bottled gas supply to the module, and (4) plant nitrogen supply (high and low pressure) to the module.

This report is available at no cost from the National Renewable Energy Laboratory at www.nrel.gov/publications.

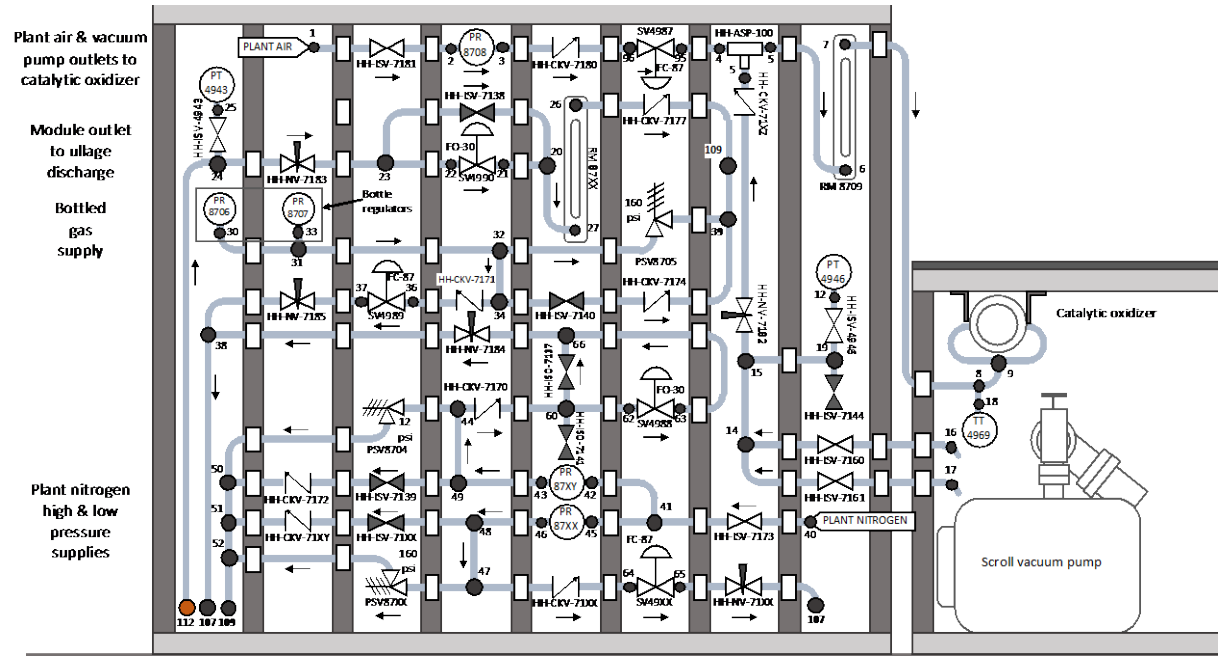

Figure 20. Manifold layout for ½" tubing

Process installation—electrical layout

The original plan was to locate the PLC, 480V to 240V stepdown transformer, distribution panels, solid-state relays for the heaters, and VFD for the compressor at the process platform shown in Figure 7. NSO decided that these components would be better located in the fire-suppression shed that was located about 60 ft from the platform and just outside the Class 1 Div 2 restricted area. This arrangement eliminated the explosion-proof requirement for these components and kept them out of the weather. The closest access to 480V 3-phase power was the maintenance building that was about 100 ft from the fire shed. NSO trenched and laid 480V 3-phase lines underground from the maintenance building to the shed. NSO installed 480V and 240V distribution panels on the inside wall of the shed, along with a 480V/240V stepdown transformer. NSO also installed enclosures for the PLC and solid-state relays, and the VFD for the headspace gas compressor inside of the shed.

Process installation—PLC with signal and control wiring

Signal sensing, process monitoring, and control was performed using a PLC. The PLC was fitted with an eight-slot module chassis, which held six analog input modules that provided channels to read temperature, pressure, and flow transmitters. The chassis held two digital output modules that provided channels to send control signals to control valves, vacuum pumps, electric heaters, and the VFD for the compressor. Figure 21 shows detail of the PLC enclosure.

This report is available at no cost from the National Renewable Energy Laboratory at www.nrel.gov/publications.

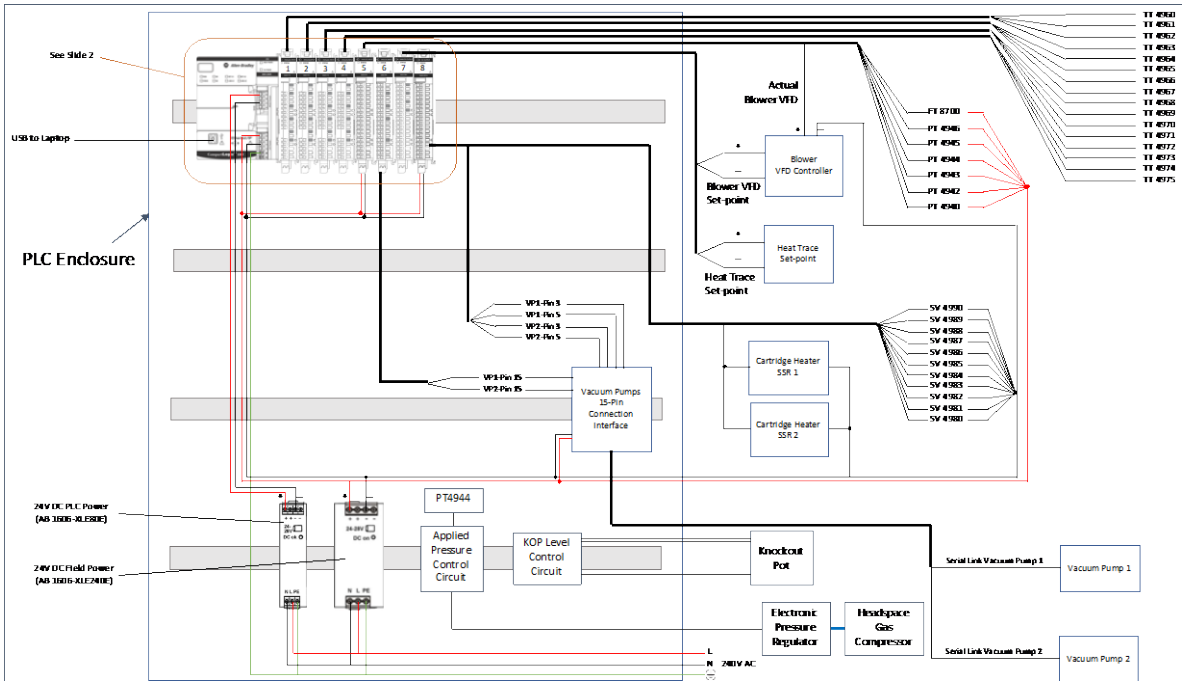

Figure 21. Schematic of sensor and communication wiring from PLC to platform

The enclosure contained the PLC and field power supplies, and custom circuits that interfaced between the PLC and equipment on the platform. Along with the solenoid valves, control signals were sent to solid-state relays for the five heat trace circuits, the two vacuum pumps, the cartridge heater for the membrane, and to the VFD for the headspace gas compressor. Figure 22 shows detail on how the signal wiring was terminated in junction boxes at the process platform according to their proximity to sensors, valves, or equipment. All wiring that is shown in Figure 22 was supported by an elevated cable tray. The cable tray kept the wiring organized and off the ground from the fire shed to the process platform. The wiring terminated in a single junction box at the platform before splitting to the individual junction boxes.

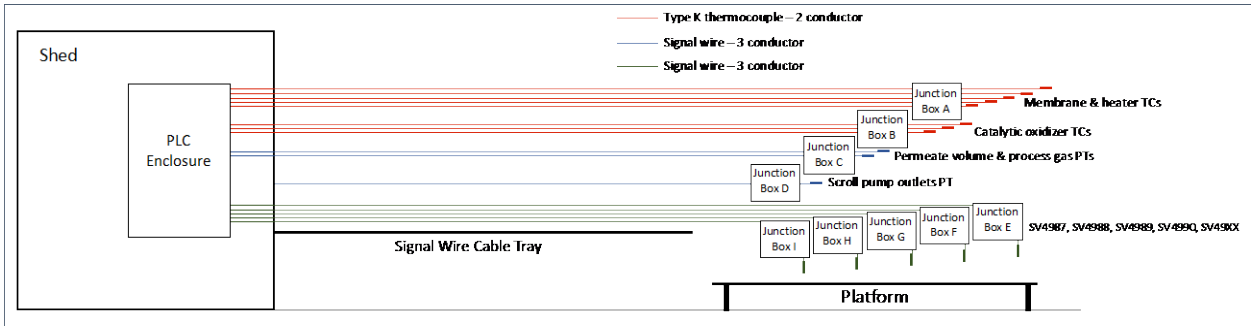

Figure 22. Schematic of sensor and communication wiring from PLC to junction boxes on the process platform

This report is available at no cost from the National Renewable Energy Laboratory at www.nrel.gov/publications.

Process installation—PLC custom circuitry

NREL fabricated several circuits that provided communication between the PLC and certain pieces of process equipment. We fabricated a circuit board to enable digital communication between the PLC and the two vacuum pumps. The circuit board interfaces the PLC input and output signals to the corresponding pins of a DB15 serial communication cable for each vacuum pump. The circuit board also converts the PLC DC output signals (VP-Pin 3 and VP-Pin 4) to "closed circuit" and "open circuit" signals, the required input signal format for the vacuum pumps. This circuit board allows the PLC to set the mode of the vacuum pumps (OFF, low speed, regular speed), and monitor the health signal of each pump.

NREL fabricated a circuit that provides signal conversion for the two level switches that start and stop HTF draining from the KOP. The circuit design is shown in Figure 23 and uses the level switch position to send a high (open) or low (closed) voltage signal to two PLC analog input channels. Ladder logic in the PLC tracks the change state sequence of the switches and sends an open or close digital signal to the solenoid valve that drains the KOP.

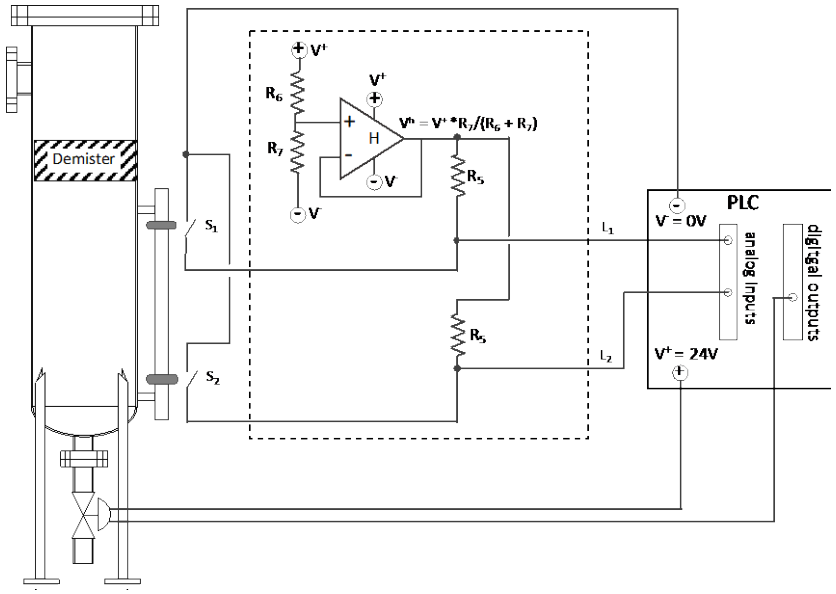

Figure 23. Circuit for conditioning level switch states and controlling drain valve

The headspace gas compressor contained a shaft seal that needed an external applied pressure that was always 5 psi greater than the headspace gas pressure inside the compressor. NREL fabricated a circuit (Figure 24) that reads the headspace gas pressure (PT4944) and provides a control signal to an electronic pressure regulator that applies nitrogen gas pressure to the compressor shaft seal. The circuit functions independent of the PLC and creates a voltage that is proportional to the headspace gas pressure and adds a constant voltage that creates a control signal that causes the electronic pressure regulator to output an applied pressure that equals the headspace gas pressure plus 5 psi.

This report is available at no cost from the National Renewable Energy Laboratory at www.nrel.gov/publications.

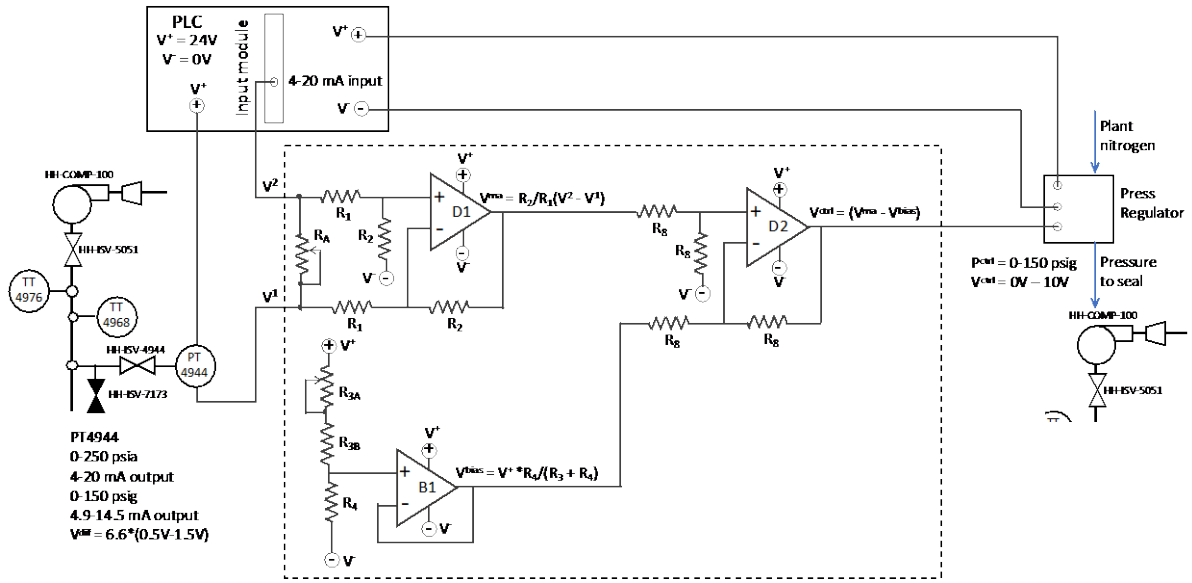

Figure 24. Control circuit for sending a signal to the electronic pressure regulator to supply nitrogen gas pressure to the compressor shaft seal

Process installation—electrical power requirements and wiring—240V and 480V
Before running 3-phase power to the process platform, we verified that our 480V current needs do not exceed the current limit (100A) supplied at 480V from the maintenance building. The headspace gas compressor was the only equipment that operated with 480V. Power and current requirements for the compressor are listed in Table 3. The required current was 21A, so we allocated 25A at 480V for the headspace gas compressor VFD shown in Figure 25.

Table 3. Electrical requirements for 480V power

Installation Components	Electrical Requirements					
	Watts	Volts	Phase	Phases used	Amps	CB
HSG compressor	15,000	480	3	ABC	21	30

Components that use 240V are listed in Table 4. Summing their current requirements by leg produced a maximum phase current of 44A at 240V, or 22A supplied at 480V. This result is much less than the 75A at 480V that is available to the stepdown transformer, so the power supplied from the maintenance building and provided to the platform was more than sufficient to provide the power needs at 480V and 240V.

This report is available at no cost from the National Renewable Energy Laboratory at www.nrel.gov/publications.

Table 4. Electrical requirements for 240V power

Test Scale Installation Components	Electrical Requirements					
	Watts	Volts	Phase	Phases used	Amps	CB
PLC modules and field power	various	240	1	BC	5	10
Cartridge heater for membrane	5,000	240	1	AC	21	30
Permeate volume vacuum pump 1	520	240	1	AB	2.2	10
Permeate volume vacuum pump 2	520	240	1	AB	2.2	10
MI cable 1	2,300	240	1	BC	9.6	15
MI cable 2	1,890	240	1	AB	7.9	10
MI cable 3	1,080	240	1	AB	4.5	6
MI cable 4	1,310	240	1	AB	5.5	10
MI cable 5	1,080	240	1	BC	4.5	6

Figure 25 shows equipment and heaters that use 480V and 240V power. Equipment includes the headspace gas compressor, the PLC and two vacuum pumps. Electrical heaters include the cartridge heater for the membrane and the five heat trace circuits for process equipment and piping.

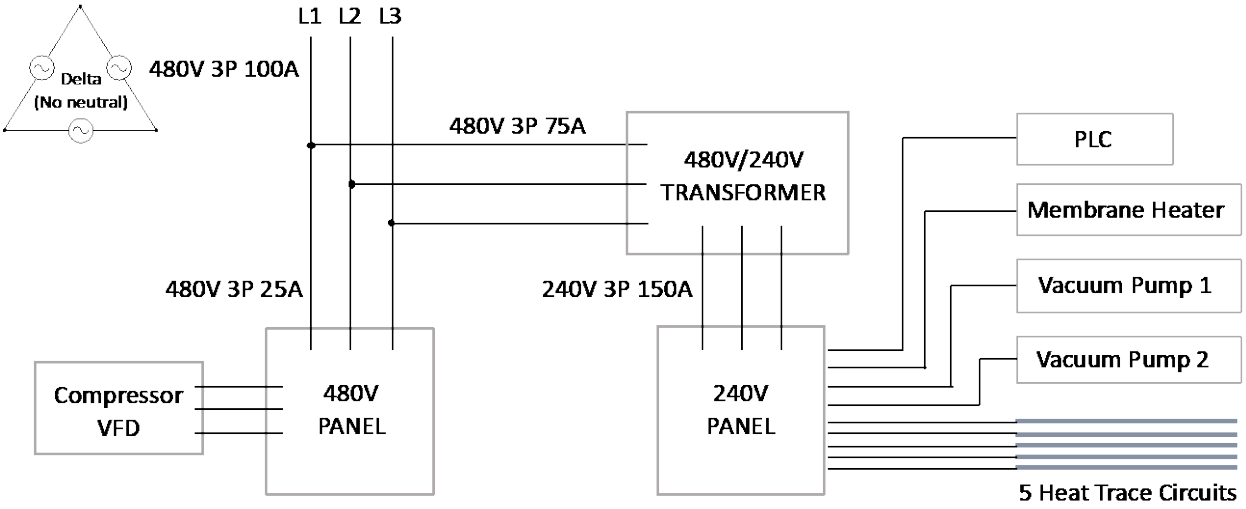

Figure 25. 480V and 240V current requirements for process installation

In addition to the signal cable tray, NSO installed a separate elevated power cable tray that ran from the fire shed to the process platform. The cable tray was mounted just below the existing piping and carried all the 240V and 480V 3-phase power wiring that is listed in Table 3 and Table 4.

This report is available at no cost from the National Renewable Energy Laboratory at www.nrel.gov/publications.

Process installation—PLC programming and process control logic

NREL programmed the PLC using its ladder logic language to create a set of standby and operating modes for daily process operation. The modes along with their logic flow from mode to mode are shown in Figure 26. Mode 0 is the shutdown mode and is used when the process is not in operation or being prepared for operation. All valves are closed, pumps and compressor are off, all heaters are off except the membrane heater, which keeps the membrane at about 200°C. When starting the process, Mode 1 is selected first and used to warm up the piping and equipment. All valves are open, so headspace gas can flow through the process piping to help warm the system. Modes 2 and 3 are the two operating modes. Mode 2 is the hydrogen extraction mode. In Mode 2, the headspace gas compressor and vacuum pumps are running and the permeate valve (SV4986) is open. Mode 3 is for hydrogen measurement. Mode 3 is the same as Mode 2 except Mode 3 has a timing routing that closes the permeate valve and measures the pressure increase in the permeate volume.

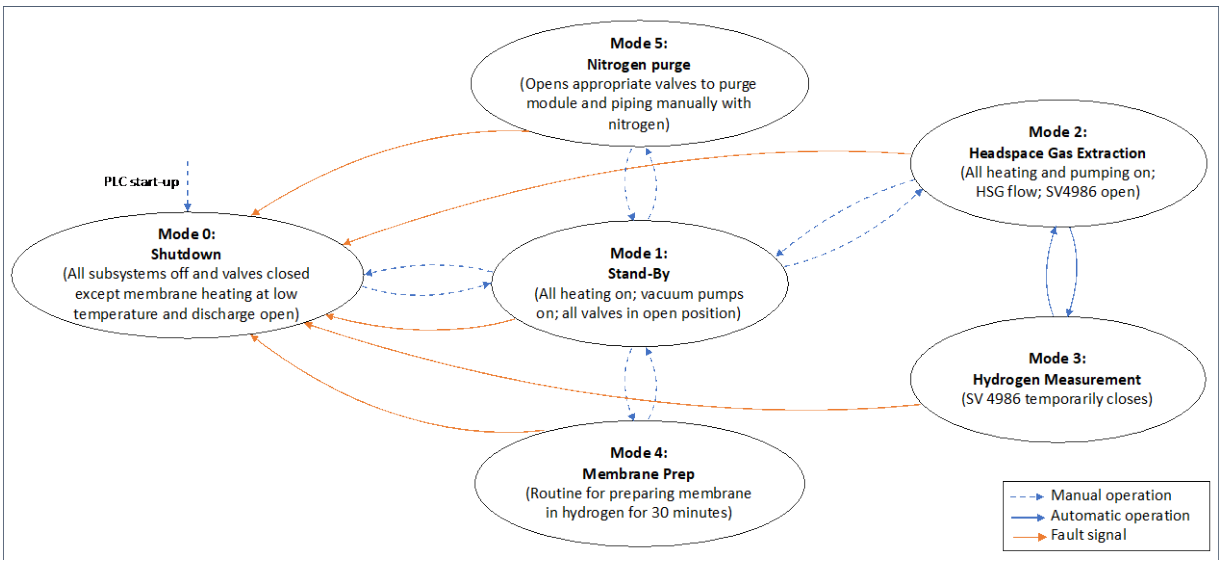

Figure 26. Standby and operating modes for PLC process control

Mode 3 returns to Mode 2 when the measurement is complete. Modes 4 and 5 are maintenance modes. Mode 4 prepares the membrane by soaking in 5% hydrogen for 30 minutes. Mode 5 allows the system to be purged with nitrogen to remove HTF condensate as needed.

The PLC did not have a user interface that allows operators to make real-time changes to the process operation, so NREL fabricated a selector box that was wall mounted next to the PLC enclosure in the fire shed. The box has a selector switch and numerical display that allowed the NSO operators to easily select modes and move between different preparation and operating steps without needing to interface with the PLC using the laptop computer. During the final four months of this TCF project, NSO used the selector box and modes to operate the process on a daily schedule.

This report is available at no cost from the National Renewable Energy Laboratory at www.nrel.gov/publications.

Process modeling—dynamic power plant model development

From March 2020 to April 2021, NREL's travel to NSO was limited to a few trips, and work on the process at the site was essentially stopped. We used some of this time to create a transient power plant model to better track hourly and monthly levels of HTF hydrogen in the solar field receivers and power block subsystems. NREL wrote the transient model to solve for hydrogen concentrations in all components of the NSO power plant that had a 2-second time step. The model used hourly HTF temperature data for the plant's solar field supply and return headers, SCA 8 loop outlets, steam generator, and expansion tanks. The transient model recorded HTF temperatures once per hour. The model generated hourly hydrogen data—24 hours per day for all components shown in Figure 27. Daily data was generated for representative days for each month of the year to produce an annual mapping of HTF hydrogen concentrations for all points within the NSO power plant.

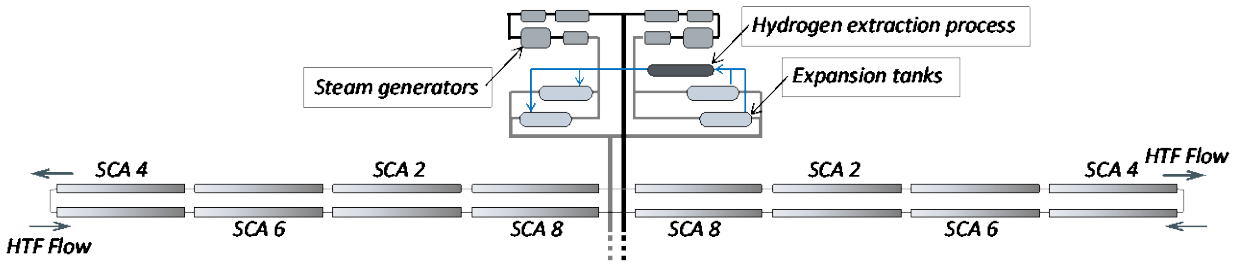

Figure 27. Power plant components in which the plant model calculates hourly HTF hydrogen levels for each month of the year

The NSO power plant model script was written in Python—an interpretive, open-source programming language. This script models hydrogen occurrence and transport within the circulating HTF of the NSO plant. The script was developed as a transient, initial value simulation, where hydrogen concentration in the circulating HTF is 0 mol/m^3 everywhere at time equal to 0 seconds. HTF circulation is modeled in time by dividing the HTF in all piping and vessels into discrete volume elements. All volume elements, dV, have the same volume that equals the HTF volume that flows past any reference point in the plant equipment or piping during one 2-second time step:

$$dV = v\,dt$$

Here v is the local HTF volumetric flow rate in the piping section or vessel, and dt is the time step. Volume elements move through the plant piping and vessels as independent packets. At the end of each time step, the volume elements move to their next positions consistent with the HTF flow direction. During each time step, hydrogen generation and permeation are calculated for each volume element according to the local HTF temperature, vessel or piping properties, and hydrogen concentration. Hydrogen concentration is updated for each volume element, dV, for that time step, dt, and the volume elements move to their next positions. Mixing between dVs does not occur except in the superheaters and steam generators, where the HTF is assumed to be completely mixed. At points where HTF flow splits, hydrogen concentration in the two split flows equal the concentration before the flow split. At points where HTF flows combine,

This report is available at no cost from the National Renewable Energy Laboratory at www.nrel.gov/publications.

hydrogen concentration in the combined flow equals the average concentration of the combined flows weighted according to their flowrates.

We used the power plant model to predict HTF hydrogen concentrations for all points in the NSO solar field and power block. We used these data to create hourly mappings of hydrogen concentrations for a base case that simulates a typical NSO operating year. We predicted annual hydrogen concentrations when the HTF has a mass fraction of 0.014 benzene and benzene derivatives. We then predicted annual hydrogen concentrations for the same conditions, but when hydrogen extraction is used to reduce hydrogen levels in the NSO plant.

Process modeling—HTF degradation rate expression

Hydrogen generation resulted from degradation of the HTF components and the degradation of benzene and benzene-like derivations which are themselves products of HTF degradation. For our plant model, we used a temperature-dependent hydrogen generation rate expression that is the sum of two terms. The first term accounts for hydrogen generation due to the decomposition of the two principal components of the HTF—biphenyl and diphenylether. The second term accounts for the decomposition of benzene and benzene derivatives; all are byproducts of HTF decomposition and are present in the circulating HTF. The derivatives included ethylbenzene, methoxybenzene, toluene, and xylene.

Decomposition rates were obtained from the literature for the HTF [21], benzene [22], ethylbenzene [23], methoxybenzene [24], toluene [25], and xylene [26]. Toluene and xylene are stable with respect to thermal decomposition at HTF operating temperatures and do not contribute significantly to hydrogen generation. Figure 28 shows the temperature-dependent decomposition rates for benzene, ethylbenzene, methoxybenzene, and new HTF. Figure 28 shows that the generation rates for these byproducts are several orders of magnitude greater than that of the HTF. Hydrogen generation due to the decomposition of benzene, ethylbenzene, and methoxybenzene accounts for most of the hydrogen that is generated in the circulating HTF once these components accumulate in the HTF. The decomposition rate of methoxybenzene is 100,000 times greater than that of the HTF, so even parts per million levels of this component in the HTF contributes to hydrogen generation rate.

To model the contribution of hydrogen generation from benzene and its derivatives, we assumed the total generation rate due these components could be represented by the temperature-dependent generation rate due to benzene only. This assumption is reasonable because benzene is the principal decomposition byproduct and the hydrogen generation rate for benzene is midway between those of ethylbenzene and methoxybenzene as shown in Figure 28. We assumed a benzene derivative mass fraction in the HTF to be 0.01 to 0.02 (1%–2%).

This report is available at no cost from the National Renewable Energy Laboratory at www.nrel.gov/publications.

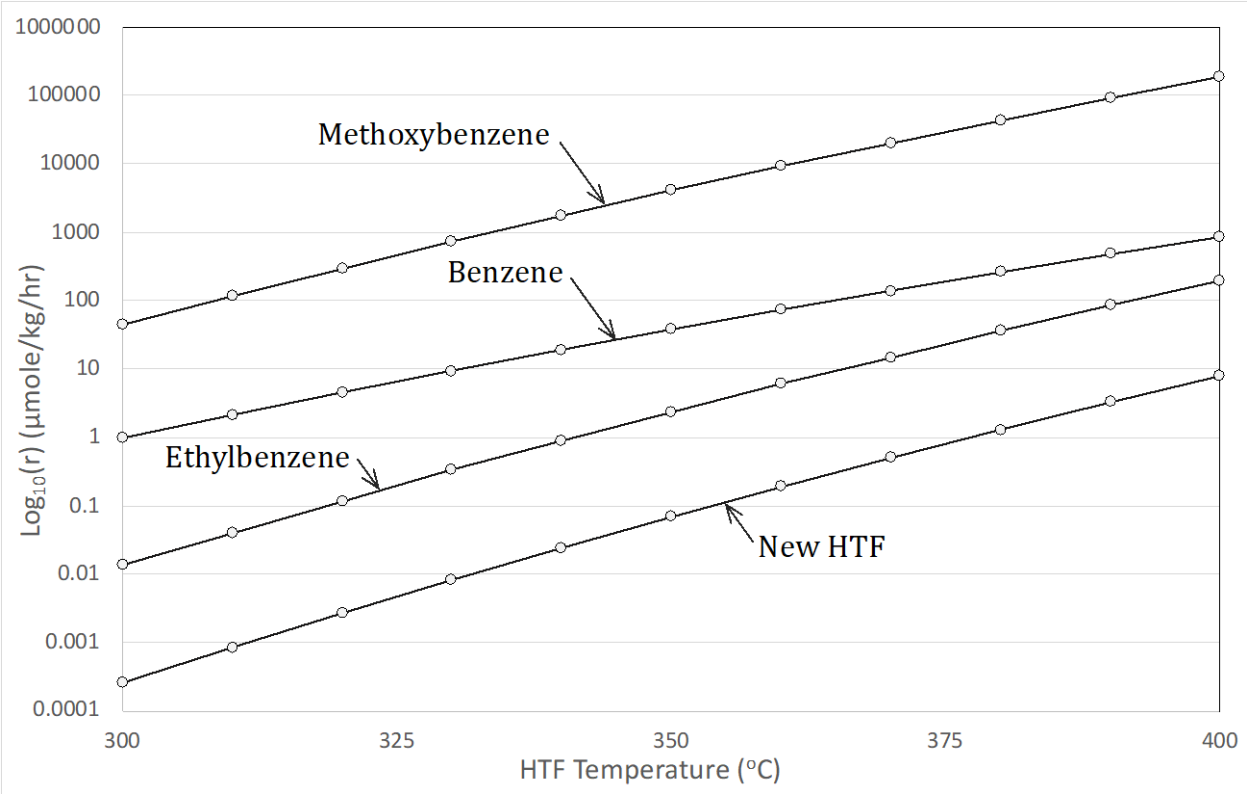

Figure 28. Comparison of degradation rates of new HTF, and benzene at HTF temperatures from 300°C to 400°C

Process modeling—receiver lifetime model development
During the pandemic, NREL developed a receiver lifetime model that predicts receiver performance by month and year for receivers in SCAs 2, 4, 6, and 8. This model was written as a Python script and uses hourly absorber temperatures and dissolved HTF hydrogen concentrations for receivers in the four SCAs, which have different HTF temperatures and hydrogen levels. Hourly dissolved hydrogen concentrations were generated by the NSO plant model by month for various operating scenarios. The model used hourly ambient and receiver absorber temperatures to estimate the getter temperature in the four SCAs.

Three physical processes determine hydrogen pressure in the receiver annulus: (1) hydrogen permeation through the absorber tube, (2) permeation through the bellows, and (3) hydrogen adsorption onto the getter. These processes are highly temperature dependent, so estimating the adsorber tube, bellows, and getter temperatures is important. Permeation through the absorber tube and getter loading are reversible, and act to increase or decrease hydrogen getter loading and annulus pressure depending on the hydrogen partial pressure in the HTF and annulus.

The receiver model used a 1-hour time step to estimate getter loading and annulus pressure in each of the four SCAs. For each time step, the model used HTF and ambient temperature data to calculate absorber tube, bellows, and getter temperatures for that time step. The model used hourly HTF hydrogen concentrations that were predicted by the NSO plant model, and annulus hydrogen pressure from the previous time step.

This report is available at no cost from the National Renewable Energy Laboratory at www.nrel.gov/publications.

With this information, the model calculated the moles of hydrogen permeating across the absorber tube and bellows during the time step. The net change in moles of hydrogen was added to or subtracted from the getter loading from the previous time step, and the hydrogen pressure was re-calculated based on the getter loading isotherm and temperature. The model used this algorithm to simulate hydrogen permeation and loading 24 hours per day, 365 days per year using monthly temperature data. The model repeated these calculations for 25 years to create a mapping of receiver getter loading and annulus hydrogen pressure for each year for the plant operating lifetime.

Process modeling—dynamic plant model results

We ran the dynamic power plant model to estimate hydrogen levels in the circulating HTF for representative days for each month of the year. For each month, we obtained hourly HTF partial pressures for the eight SCAs in the north and south field receiver loops. The differences between north and south field SCAs were negligible. We plotted hourly HTF hydrogen partial pressures for SCA 8, because that SCA sees the highest HTF temperature.

We ran cases for several mole fractions for the benzene derivatives in the range of 0.01 to 0.02. Results showed the same monthly trends and a mole fraction of 0.014 produced very high HTF hydrogen partial pressures in May and June and very low partial pressures in November, December, and January. These results are consistent with measurements that were made at NSO during the past several years. Figure 29 shows modeled hourly HTF hydrogen for SCA 8 with no extraction for the months of May and June.

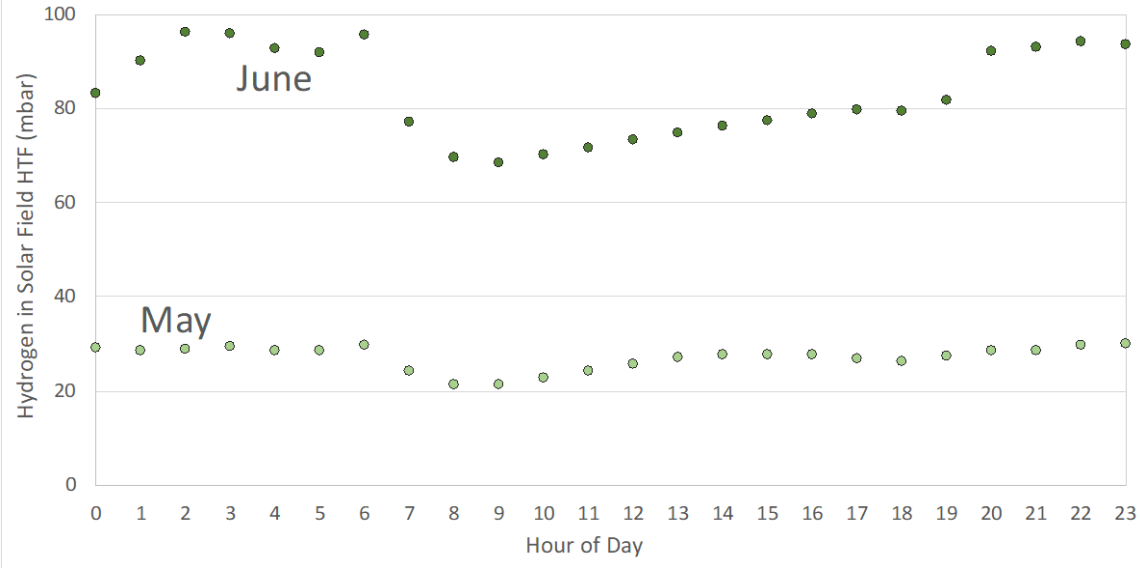

Figure 29. Hourly hydrogen levels in HTF flowing through SCA 8 receivers; model assumes HTF with 1.4% benzene-like derivatives, and no hydrogen extraction

June showed hourly HTF hydrogen partial pressures approaching 100 mbar, which is greater than typical summer values that are more in the range of 25 mbar to 75 mbar. These same conditions predicted essentially no HTF hydrogen during the winter months, due to shorter days, lower HTF temperatures, and the extreme temperature dependence of the reaction rates shown in

This report is available at no cost from the National Renewable Energy Laboratory at www.nrel.gov/publications.

Figure 28. With these model conditions and results, we concluded that we captured the full seasonal variability of HTF hydrogen levels that have been observed at the NSO power plant.

Figure 30 shows the HTF hydrogen partial pressures for May and June using the same modeling conditions except with hydrogen extraction at the rates that were predicted by the extraction process model for the final process installation. Hydrogen levels are reduced by 85% to 90% and the benefit of continuing extraction into the evening and night after the plant shuts down is clear. Hydrogen levels continue to decrease through the night and in the early morning until the plant starts up at 8 am.

Figure 31 summarizes HTF hydrogen averages for each month for the extraction and no extraction cases. The average reductions in hydrogen also were about 85% when extraction is used compared to the no extraction cases. The values shown for the months of November, December, and January were negligible for the no extraction case, so extraction during these months does not provide any benefit. The June and August averages were unexpectedly low for summertime temperatures. During discussions with NSO, they said during the months of July and August 2017—when the data were collected—the plant was shut down much of the time due to mechanical problems and repairs. This limited operating time explains the low hydrogen levels.

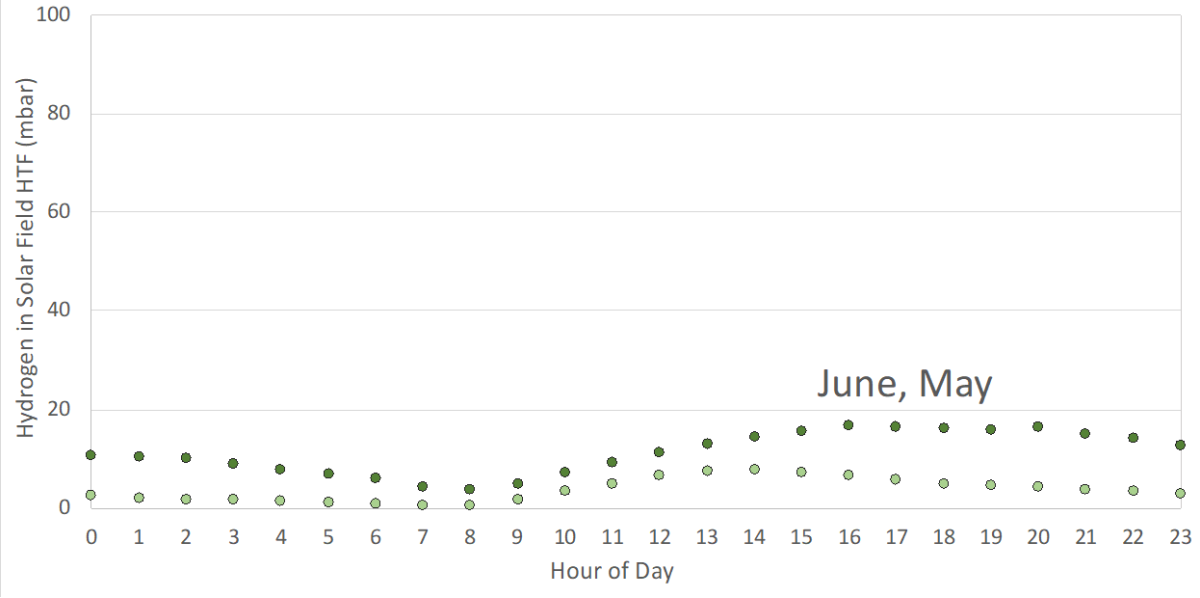

Figure 30. Hourly hydrogen levels in HTF flowing through SCA 8 receivers; model assumes HTF with 1.4% benzene-like derivatives, and with hydrogen extraction

This report is available at no cost from the National Renewable Energy Laboratory at www.nrel.gov/publications.

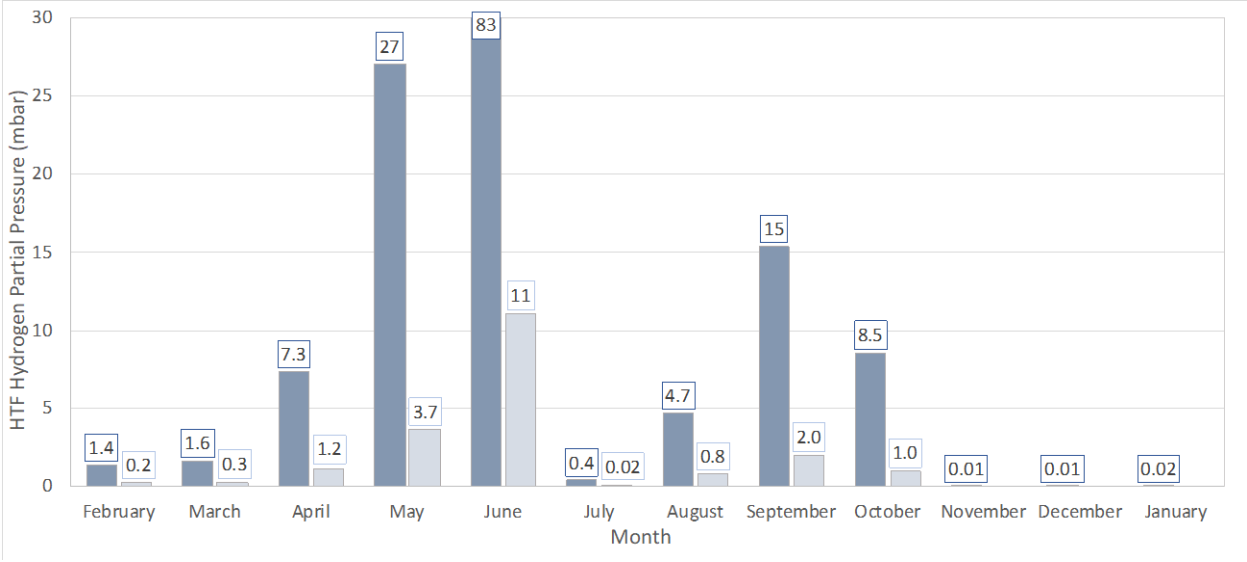

Figure 31. Average monthly hydrogen levels in HTF flowing through SCA 8 receivers (model assumes HTF with 1.4% benzene-like derivatives) with and without hydrogen extraction

We used the monthly/hourly HTF hydrogen partial pressures that were generated by the dynamic plant model as inputs to the receiver lifetime model to predict receiver performance loss for 25 operating years according to SCA position in the loops. Figure 32 shows receiver annulus hydrogen pressures for each year for SCAs 2, 4, 6, and 8.

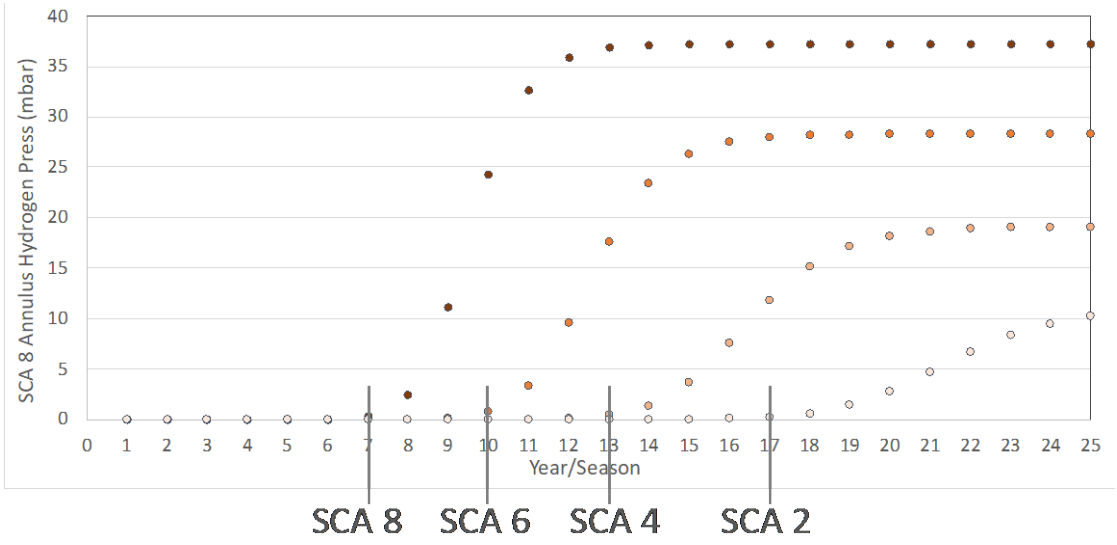

Figure 32. Annual hydrogen levels in SCA 2, 4, 6, and 8 receiver annulus—no hydrogen extraction

The receiver getters in each SCA remove hydrogen for a certain number or years before saturating, which causes increasing hydrogen pressure in the receiver's annulus. SCA 8 receivers show elevated annulus hydrogen beginning in year 7. SCA 6 begins in year 10. SCA 4 begins in year 13. SCA 2 begins in year 17. This pattern is due to increasing getter temperatures and lower getter capacities going from SCA 2 to SCA 8. Figure 33 shows the same results for receivers in

This report is available at no cost from the National Renewable Energy Laboratory at www.nrel.gov/publications.

SCAs 2, 4, 6, and 8 but with hydrogen extraction starting in year 1. For this case, SCAs 2 and 4 retain their performance for the full 25 operating years of the plant. SCA 6 begins to have elevated hydrogen in year 21, and SCA 8 in year 15. These results showed a dramatic improvement in receiver lifetimes when hydrogen extraction is used starting from the first year of operation.

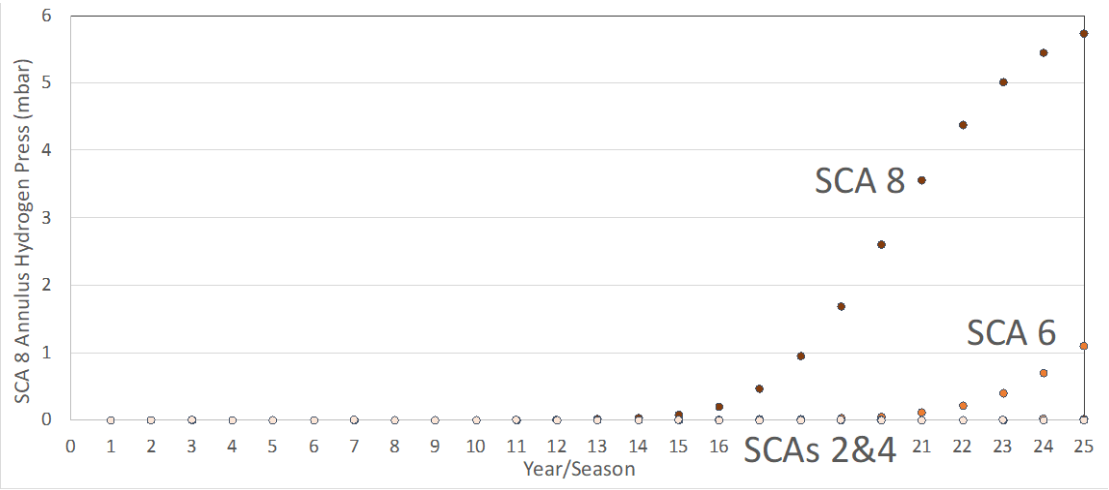

Figure 33. Annual hydrogen levels in SCA 2, 4, 6, and 8 receiver annulus—with hydrogen extraction

During NREL's last trip to NSO in November 2021, we made several measurements of HTF hydrogen in the expansion tank headspace gas. Measured hydrogen was less than 0.2 mbar for all measurements. These results are consistent with the plant model predictions that there is no hydrogen in the HTF during November, December, and January. With these results, NSO decided to shut down the process until February 2022, when hydrogen levels are expected in return to measurable levels.

NREL estimated HTF hydrogen levels for the first half of 2022 with and without extraction. Our modeling shows that we should be able to detect the improvement expected for March, since the resolution of the pressure transmitter is 0.2 mbar. We will certainly be able to detect improvement in April. We will use these results as final confirmation that the process is working properly.

Process commissioning—startup and operating problems
During March and April 2020, NSO operated the process intermittently with limited success. During this time, we worked through a series of operating control issues related to proper temperature management and headspace gas flow control. In May 2020, NSO began operating the process on a daily schedule. NSO operated the process for four weeks, which ended when they started getting overpressure readings in the permeate volume. NREL had programmed the PLC to shut down the process if permeate pressure exceeded 200 mbar. This condition indicated a leak in the membrane that was causing the excess pressure.

During our next trip to NSO, we removed the membrane assembly from the module to inspect it for leaks. The membrane had developed a pinhole size hole that required brazing to repair. We

This report is available at no cost from the National Renewable Energy Laboratory at www.nrel.gov/publications.

arranged for the NREL technician, who had performed the original brazing to travel to NSO to make the repair. The following week, when he attempted to braze the hole, the braze did not wet the membrane surface and the repair failed. This condition was caused by a film of HTF that had leaked through the pin hole, accumulated on the inside surface of the membrane, and was contaminating the braze surface.

NREL wrote a subroutine for the PLC that maintained the membrane at high temperature and allowed the HTF to vaporize off the inside surface. NSO used this routine to keep the membrane at high temperature for ten days. NREL returned and successfully repaired the membrane on their second attempt. To prevent repeated damage to the membrane when it is being removed from the module, NREL fabricated a guard ring that fit onto the free end of the membrane assembly and prevented the membrane from contacting the module wall when it was being removed or inserted. Testing after this repair did not result in any overpressure conditions.

The HTF film that deposited on the inside membrane surface was caused by liquid HTF leaking through the hole in the membrane. For this to happen, the module had to be flooded with liquid HTF, and the membrane was fully immersed in HTF. This condition was caused by HTF vapor condensing in the piping and pooling in the module during process startup, when the piping was not yet up to temperature. In April, NSO had installed drain lines in the process piping and in the module to drain HTF from the process. The piping drain lines worked but the drain line on the module was installed at the vertical midpoint of the module, so the bottom half of the module remained filled with HTF even when the drain was open.

To fix this problem, NREL fabricated an insert that fit between two gaskets and two flanges that seals the membrane assembly to the end of the module. The insert had a ½" drain port and tubing located at its bottom, so the module would drain completely, when the drain line valve was open. NREL and NSO had considered drilling a new penetration and welding a fitting into the bottom of the module, but this modification would have required the module to be retested and recertified as an ASME pressure vessel. The insert allowed the module to drain properly and did not require the module to be recertified.

With the module draining properly, we were confident that the membrane would not be immersed in HTF during startup and daily operation. Another problem that developed during this series of problems was condensation of HTF liquid in the vacuum tubing and vacuum pumps due to the leak. We spent several days purging the vacuum pumps, but the minimum vacuum still remained high. We believed that the vacuum tubing also had been contaminated with HTF and so broke apart the vacuum tubing and cleaned it. In addition, we replaced the o-rings that sealed the joints between the vacuum tube sections. With all the vacuum tubing cleaned and o-rings replaced, we recovered a system that sealed properly and pumped down to its expected vacuum. By August, we had fixed all these problems and were starting to extract hydrogen and measure hydrogen partial pressures with some consistency and confidence.

Process commissioning—process operation and hydrogen measurements
NSO began operating the process again in August 2021. During that month, NREL operated the process and made a series of headspace gas hydrogen measurements. Before circulating headspace gas through the separation module, we treated the membrane with 5% hydrogen in nitrogen for 1 hour. We filled the module with the gas mixture to 1.2 bar with the permeate valve

This report is available at no cost from the National Renewable Energy Laboratory at www.nrel.gov/publications.

closed, so the hydrogen would partition and remain in the module and permeate volumes. The hydrogen partial pressure at 1.2 bar is 60 mbar. This treatment removes silver oxide and other oxides from the palladium/silver alloy surface and facilitates the transfer of hydrogen through the membrane.

At the end of the treatment, we removed most of the hydrogen by opening the permeate valve. We closed the permeate valve and measured the remaining hydrogen in the module by recording the pressure increase in the permeate volume. Figure 34 shows permeate volume pressure increase during measurement of hydrogen partial pressure in the module. The plot has the initial rapid increase followed by leveling off that is expected for these measurements. The final pressure in the permeate volume and module was 2.4 mbar.

After finishing the membrane treatment, we started the process by circulating headspace gas through the module using the headspace gas compressor. We measured hydrogen in the headspace gas at three different times that day. The weather that day was partly cloudy. The plant operated during daylight hours, but the direct sunlight was interrupted several times during afternoon operation.

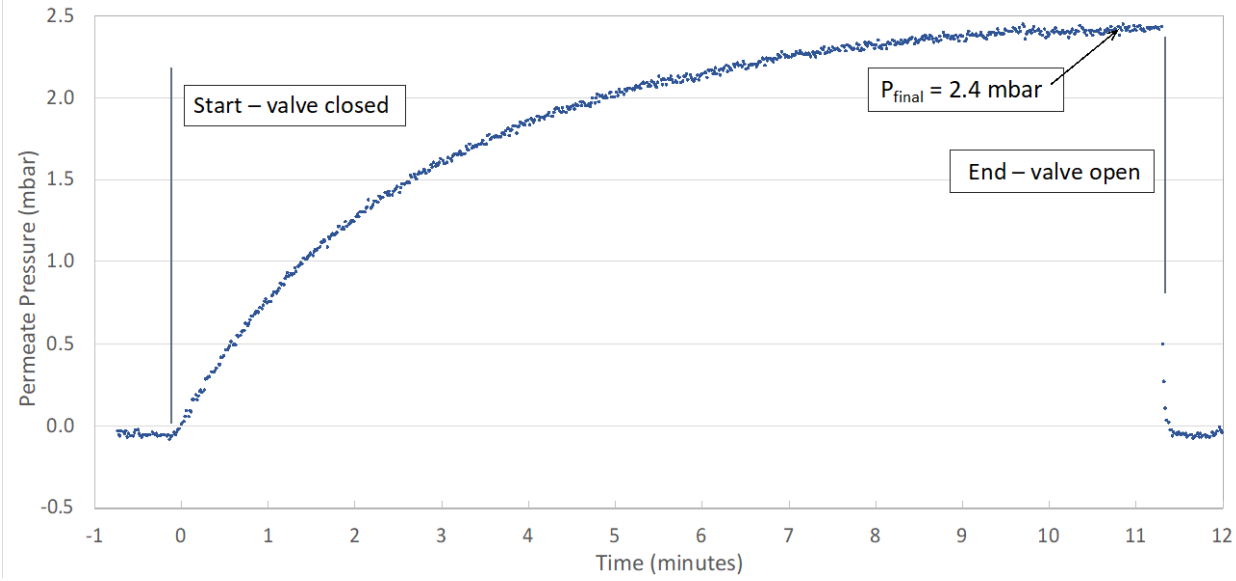

Figure 34. Permeate pressure versus time for measuring hydrogen in the module after treating the membrane with 5% hydrogen in nitrogen

These three measurements had similar pressure responses. The pressure increased nicely and leveled off as expected. We observed signal drift especially during periods of intermittent clouds or when shadows from the structural pillars brought the transmitter in and out of direct sunlight. Final pressures ranged from 2.5 mbar to 3.6 mbar. Our plant modeling showed that hydrogen levels in the headspace gas can vary several mbar during the course of day, and the pressures tend to increase in the evening after the plant has shut down before decreasing after midnight. Overall, the measurements were reasonable for an early fall operating day that experienced clouds in the late morning and afternoon.

This report is available at no cost from the National Renewable Energy Laboratory at www.nrel.gov/publications.

NSO asked NREL to provide a measurement that was independent of the permeate pressure increase that confirmed that the process is actually extracting hydrogen from the headspace gas. We used the data in Figure 35 to confirm that hydrogen was extracted and oxidized to water vapor in the catalytic oxidizer. In Figure 35, hydrogen pressure data were plotted to show when the permeate valve was opened and hydrogen was pumped out of the permeate volume and sent to the catalytic oxidizer. After a 15-second delay, the catalytic oxidizer temperatures increased indicating that hydrogen was being oxidized to water vapor in the oxidizer. These plots confirmed that the process is extracting hydrogen from the headspace gas.

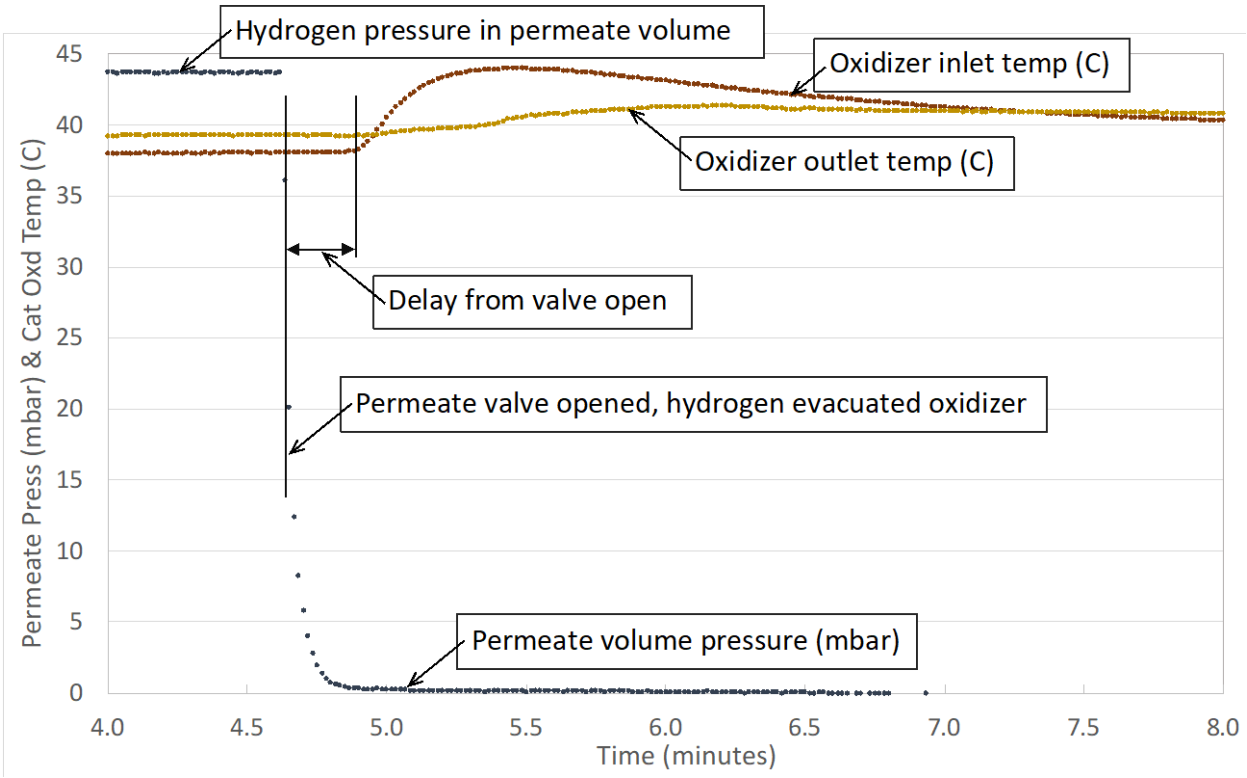

Figure 35. Catalytic oxidizer temperature response when hydrogen is withdrawn from the permeate volume and passed through the oxidizer

Technology marketing—licensing

Starting in the fall of 2020, NREL engaged in discussions and negotiations with two companies who were interested in licensing the technology from NREL and providing the process to other parabolic trough power plants around the world. Both companies considered Spain as the best market to begin installing this process in CSP plants due to the large number of plants (40) and the relative uniformity of their plant designs. As of the end of 2021, one of the two companies agreed to licensing terms, and they plan to sign the agreement in early 2022. This agreement will allow this company to begin process installations in 2022. NREL and the licensee have received many requests for information and status of the technology. Requests have come from parabolic trough owners and operators in Spain, Morocco, Dubai, and South Africa, as well as the Spanish CSP trade organization.

This report is available at no cost from the National Renewable Energy Laboratory at www.nrel.gov/publications.

6 TCF Project Continuing Work

Continuing work and monitoring at NSO
This project lost 15 months due to the COVID-19 pandemic. Additional time was lost due to the inefficiencies associated with starting work again on a project that was idle for many months. Process startup during the summer of 2021 was delayed by several problems with braze contamination, o-ring degradation, and condensates in the vacuum pumps that started with a membrane leak and required several months to work through and fix. Still, at the end of this project we have a working process and are ready to determine process performance in the first half of 2022.

The project PI, Greg Glatzmaier, left NREL in early 2022 and continues to work at the NSO plant in 2022 to refine the process operating procedures, determine process performance and the impact on the NSO solar field. NREL estimated HTF hydrogen levels for the first half of 2022 with and without extraction. We will be able to detect the improvement predicted for February and certainly March, since the resolution of the pressure transmitter is 0.2 mbar.

Process implementation in Spanish parabolic trough power plants
NREL and the licensee expect to complete and sign the licensing agreement for use of the technology in early 2022. Next, the licensee will work to design and implement the hydrogen mitigation process in a Spanish power plant. Greg Glatzmaier, the project PI, will provide technical support to the licensee for the first few installations to ensure that all practical knowledge is transferred to the company. The licensee expects to complete its first process installation by the end of 2022.

7 TCF Project Summary

Fundamental advances
This technology development effort consisted of two CRADAs between NREL and AE. The first CRADA was funded by AE and DOE's Solar Energy Technologies Office (SETO). This work effort focused on power plant, process, and receiver modeling, analysis, and experiments at NREL. The key outcome was the development and laboratory demonstration of an integrated process that extracts hydrogen from a gas mixture and measures the partial pressure and molar extraction rate of hydrogen. The second CRADA was funded by AE and the DOE TCF. This work focused on the design, engineering, procurement, installation, and testing of the hydrogen mitigation process at the Nevada Solar One power plant in Boulder City, Nevada. These two CRADAs produced many fundamental advances. Advances that were realized in the first SETO CRADA were:

- A simple hydrogen sensor that measures hydrogen partial pressure in the expansion tank headspace gas at expansion tank conditions
- Extended receiver heating and heat loss measurements that provided the first evidence that hydrogen permeation in receivers is reversible and that receiver performance can be improved with extended receiver heating when no hydrogen is present in the absorber
- A power plant hydrogen transport and generation model that showed that controlling hydrogen levels in the expansion tanks maintains the level of dissolved hydrogen in the HTF that is circulating in the collector field to target levels

This report is available at no cost from the National Renewable Energy Laboratory at www.nrel.gov/publications.

- A receiver lifetime model that estimated the years that a receiver would last in the collector field as a function of SCA position and dissolved hydrogen concentration in the circulating HTF
- Modeling and experimental testing that generated critical partitioning and mass transfer coefficients for hydrogen at the HTF liquid/gas interface within the expansion tanks
- An integrated hydrogen separator and sensor module design that separates hydrogen from the headspace gas, measures hydrogen partial pressure in the headspace gas, and measures the molar rate of hydrogen extraction from the expansion tank headspace gas.

The advances that were achieved in the first CRADA served as the design basis for the process installation that was the purpose of the second CRADA. In this way, all effort that was made in the first SETO CRADA was used to advance and complete the development of this technology in the second CRADA.

Achievements that were realized in the second TCF CRADA were:

- A process configuration and location that was manageable and did not interfere with the day-to-day operation of the NSO power plant
- Successful procurement of major equipment, instrumentation, and contracting services that met the requirements for installation in a Class I Division II restricted area
- Successful design and third-party fabrication of custom vessels that were certified to meet ASME Pressure Codes
- First-of-a-kind installation and testing of a complex mitigation process without any safety- or accident-related events
- Successful completion of process commissioning while managing work delays caused the COVID-19 pandemic
- First real-time measurements of hydrogen partial pressure in the headspace gas of expansion tanks at a parabolic trough power plant
- A successful collaboration between NREL and NSO staff over a period of several years to complete all design, procurement, installation, and commissioning tasks without help from an EPC
- Follow-on plans to track the performance of the process that was installed at NSO
- Follow-on plans to license the technology to an engineering services company and to install the same process at power plants in the United States, Spain, North Africa, South Africa, and the Middle East.

This report is available at no cost from the National Renewable Energy Laboratory at www.nrel.gov/publications.

References

[1] http://www.nrel.gov/csp/solarpaces/

[2] L. Moens, D. Blake (2008) "Mechanism of hydrogen formation in solar parabolic trough receivers," NREL/TP-510-42468.

[3] B. Johns, E. A. McElhill, J. O. Smith (1962) "Thermal Stability of Some Organic Compounds," J. of Chemical and Engineering Data 7(2) 277-281.

[4] K. Horikawa, H. Okada, H. Kobayashi, W. Urushihara (2009) "Hydrogen Permeation Estimated by HMT in Carbon Steel Exposed to Gaseous Hydrogen," Materials Transactions 50(9), 2201–2206.

[5] V. L. Gadgeel, D. L. Johnson (1979) "Gas-Phase Hydrogen Permeation and Diffusion in Carbon Steels as a Function of Carbon Content from 500 to 900 K," J. Materials for Energy Systems 1(2), 32–40.

[6] J. Labaton, Y. Harats (1989) "Hydrogen Pump," U.S. Patent No. 4,886,048.

[7] D. Alique, D. Martinez-Diaz, R. Sanz, J. A. Calles (2018) "Review of Supported Pd-Based Membranes Preparation by Electroless Plating for Ultra-Pure Hydrogen Production," Membranes 8, 5; doi: 10.3390/ membranes 8010005.

[8] O. Sohr, M. Mollenhoff, T. Kuckelkorn (2013) "Laser induced release of encapsulated noble gas in Schott receiver," 2013 Solar PACES Conference.

[9] F. Burkholder, M. Brandemuehl, C. Kutscher, E. Wolfrum (2008) "Heat conduction of inert gas-hydrogen mixtures in parabolic trough receivers," Proceedings of the ASME 2nd International Conference on Energy Sustainability, ES2008-54176.

[10] G. C. Glatzmaier (2013) "Systems and methods for selective hydrogen transport and measurement." U.S. Patent 8,568,582.

[11] G. C. Glatzmaier (2020) "Acciona power plant hydrogen mitigation project," NREL Technical Report NREL/TP-5500-73168.

[12] G. C. Glatzmaier, D. A. Cooney (2017) "Sensor for measuring hydrogen partial pressure in parabolic trough power plant expansion tanks." AIP Conference Proceedings 1850, 020007: doi: 10.1063/1.4984331.

[13] G. C. Glatzmaier (2018) "Hydrogen sensor for parabolic trough expansion tanks," AIP Conference Proceedings 2033, 030006; doi: 10.1063/1.5067022.

[14] G. C. Glatzmaier, R. Cable, M. Newmarker (2017) "Long-term heating to improve receiver performance." AIP Conference Proceedings 1850, 020006: doi: 10.1063/1.4984330.

This report is available at no cost from the National Renewable Energy Laboratory at www.nrel.gov/publications.

[15] G. C. Glatzmaier, R. Cable, M. Newmarker (2017) "Steady-state plant model to predict hydrogen levels in power plant components." AIP Conference Proceedings 1850, 020008: doi: 10.1063/1.4984332.

[16] K. F. Beckers, G. C. Glatzmaier (2018) "Modeling and simulating diffused aeration for hydrogen removal from expansion tanks of parabolic trough solar thermal power plants," AIP Conference Proceedings 2033, 030001; doi: 10.1063/1.5067017.

[17] G. C. Glatzmaier, "Hydrogen sensing and separation," U.S. Patent No. 10,646,821 (2020).

[18] G. C. Glatzmaier, "Integrated hydrogen sensor and separator for parabolic trough expansion tanks," AIP Conference Proceedings 2126, 120007 (2019). doi: 10.1063/1.5117625.

[19] K. F. Beckers, G. C. Glatzmaier (2018) "Experimental measurements of Henry's law constant and mass transfer coefficient of hydrogen absorbing in eutectic BP/DPE heat transfer fluid," Solar Energy 173, 304–312.

[20] MathWorks (2012). MATLAB Release 2012a, The Mathworks, Inc., Natick, Massachusetts, United States.

[21] T. Kuckelkorn, C. Jung, T. Gnädig, C. Lang, C. Schall (2016) "Hydrogen Generation in CSP Plants and Maintenance of DPO/BP Heat Transfer Fluids – A Simulation Approach," AIP Conf. Proceedings 1734, 090002; doi: 10.1063/1.4949187.

[22] K. Hou, B. Palmer (1965) "The Kinetics of Thermal Decomposition of Benzene in a Flow System," J. Phys. Chem. 69 (3), 863-868.

[23] W. Muller-Markgraf, J. Troe (1988) "Thermal Decomposition of Ethylbenzene, Styrene, and Bromophenylethane," J. Phys. Chem. 92(17), 4914-4922.

[24] J. Mackie, K. Doolan, P. Nelson (1989) "Kinetics of the Thermal Decomposition of Methoxybenzene (Anisole)," J. Phys. Chem. 93(2), 664-670.

[25] M. Oehlschlaeger, D. Davidson, R. Hanson (2007) "Thermal Decomposition of Toluene: Overall Rate and Branching Ratio," Proceedings of the Combustion Institute 31, 211–219.

[26] H. Hippler, S. Seiseland, J. Troe (1994) "Pyrolysis of p-Xylene and of 4-Methylbenzyl Radicals," 25th International Symposium on Combustion, 875-882.

This report is available at no cost from the National Renewable Energy Laboratory at www.nrel.gov/publications.